ILLITIZATION OF DIAGENETIC KAOLINITE-TO-DICKITE CONVERSION SERIES: LATE-STAGE DIAGENESIS OF THE LOWER PERMIAN ROTLIEGEND SANDSTONE RESERVOIR, OFFSHORE OF THE NETHERLANDS

BRUNO LANSON[1], DANIEL BEAUFORT[2], GILLES BERGER[3], JULIEN BARADAT[4], AND JEAN-CLAUDE LACHARPAGNE[4]

[1] *Environmental Geochemistry Group, LGIT IRIGM, URA 733 CNRS, BP 53, 38041 Grenoble cedex 9, France*

[2] *Laboratoire de pétrologie des altérations hydrothermales, URA 721 CNRS, Université de Poitiers, 40 avenue du recteur Pineau, 86022 Poitiers cedex, France*

[3] *Laboratoire de géochimie, URA 067 CNRS, Université Paul Sabatier, 38 rue des 36 ponts, 31054 Toulouse, France*

[4] *Elf Aquitaine Production, CSTJF, 64018 Pau cedex, France*

ABSTRACT: **This paper describes the diagenetic evolution of clay minerals in the Rotliegend sandstone reservoir under contrasting burial histories in the Broad Fourteens basin (Dutch sector, Southern North Sea). The diagenetic modifications affecting the crystal structure of clay minerals (both kaolin-group and illitic minerals) were studied using X-ray diffraction (XRD). The XRD study includes oriented and random mounts of various size fractions, numerical processing (decomposition) of XRD profiles, and simulation of one-dimensional and three-dimensional XRD patterns. Petrographic observations, differential thermal analysis, K/Ar geochronology, and geochemical considerations complement the XRD study and allow determination of the sequence of mineral crystallization and the morphological evolution of clay minerals and place further constraints on the absolute timing of diagenetic events and on the nature of the fluids responsible for clay-mineral crystallization.**

From deposition time (~ 275 Ma) to the Kimmerian orogeny (~ 155 Ma), crystallization of kaolinite at the expense of K-feldspars was favored by acid fluids from the underlying Carboniferous Coal Measures source rocks; kaolinite crystallization is followed by a steady kaolinite-to-dickite transformation affecting both the structure and the morphology of kaolin-group minerals. The structural characteristics of kaolin-group minerals are related to the burial history of the sediments prior to the Kimmerian orogeny. During the Kimmerian orogeny, rapid illitization of kaolin-group minerals was favored both by increased heat flow in the sedimentary pile and by widespread presence of faults, which permitted significant fluid flow probably from the Zechstein Formation. The morphological and structural characteristics of illitic minerals, i.e., illite content of illite/smectite mixed layer (I/S), ratio of illite to I/S, and three-dimensional structure of illitic minerals, do not represent the progress of a smectite-to-illite transformation, but these characteristics clearly reflect the temperature during illitization of kaolin.

INTRODUCTION

Diagenetic evolution of clay minerals has been extensively described for over twenty-five years by many authors. X-ray diffraction (XRD) has been the essential tool to reveal the diagenetic sequences of clay-mineral transformations. In diagenesis, smectite illitization has been documented mostly in Gulf-Coast-type basins, where shales make up the bulk of the stratigraphic section (Burst 1969; Perry and Hower 1972; Hower et al. 1976; Środoń 1979, 1984a; Velde et al. 1986; Glasmann et al. 1989; among many others). In addition to being lithologically homogeneous, shales are an essentially chemically closed system (Hower et al. 1976). Indeed, no major systematic variation in bulk composition has been observed for argillaceous samples as a function of depth (Dunoyer de Segonzac 1970; Perry and Hower 1970; Weaver and Beck 1971; Hower et al. 1976).

More recently, diagenetic evolution of clay minerals has been studied in sandstones, especially in the North Sea, because of the influence of both their mineralogy and their morphology on reservoir petrophysical properties such as permeability (Seeman 1982; Rossel 1982; McHardy et al. 1982; Morris and Shepperd 1982; Pye and Krinsley 1986; Thomas 1986; Howard 1992). Additionally, the diagenetic evolution of clay minerals has been used for oil and gas exploration, either for stratigraphic correlations (Fisher and Jeans 1982) or to determine the timing of clay-mineral emplacement in response to complex burial history and to resulting porewater chemistry (Burley 1984; Kantorowicz 1984; Goodchild and Whitaker 1986; Burley and Flisch 1989). Migration of fluids each with a different composition, in particular those coming from source rocks, induce parageneses more diverse than those in shales (Hoffman and Hower 1979), and usually fairly complex sequences of clay-mineral (and non-clay-mineral) neoformation (see Bjørlykke and Aagaard 1992, for a review of diagenetic schemes proposed for North Sea reservoirs). For example, the various morphologies of kaolin-group minerals (Throughout the paper the term "kaolin" is used to describe kaolin-group minerals without specification of the polytype, whereas "kaolinite" refers specifically to the polytype) are usually presented as resulting from different crystallization episodes (Bjørlykke and Aagaard 1992) with major implications for porewater geochemistry (e.g., reservoir flushing).

With increasing temperature conditions, a morphological change has been described for both illitic and kaolin-group minerals from scanning electron microscope (SEM) observations (Güven et al. 1980; Pollastro 1985; Keller et al. 1986; Inoue 1986; Ehrenberg et al. 1993; Kantorowicz 1984; Thomas 1986) and transmission electron microscope (TEM) observations (Inoue 1986; Inoue et al. 1987; Inoue et al. 1988; Glasmann et al. 1989; Lanson and Champion 1991). Whatever the geological environment (hydrothermal, geothermal, or diagenetic) and to a first rough approximation, illitic minerals have mostly flaky habits when randomly interstratified illite/smectite mixed layer (I/S) is dominant, hair-like or lath-shaped particles when ordered I/S dominates, and mainly platy particles when end-member illite becomes the essential phase. In diagenesis, the morphology of kaolin-group minerals also changes from vermicular aggregates to blockier crystals along with their polytype modification from kaolinite to dickite (Ehrenberg et al. 1993; McAulay et al. 1993). Although related, both morphological and structural transitions are not strictly interdependent. The morphological change has been observed in various reservoir formations of the North Sea (Kantorowicz 1984; Thomas 1986; Osborne et al. 1994), but the kaolin polytype modification was not investigated.

Along with the morphological changes, and probably at their origin, the structure of these clay minerals is modified. In both shale-dominated and sandstone-dominated environments, clay mineral structure is usually studied by X-ray diffraction on oriented preparations of clay separates. Consequently, structural information is restricted to one dimension along the c^* axis, i.e., in the case of mixed-layer illite/smectite, relative proportions of smectite and illite layers, as well as the ordering type of the I/S. However, because the crystal morphology depends not on the stacking sequence of individual layers but on the three-dimensional (3-D) structure of elementary layers, the usual approach needs to be complemented with study

JOURNAL OF SEDIMENTARY RESEARCH, VOL. 66, NO. 3, MAY, 1996, P. 501–518
 1073-130X/96/066-501/$03.00

of clay-mineral structure by X-ray diffraction on randomly oriented powders. The evolution of the 3-D structure of illitic material from a hydrothermal environment has been reported previously by Drits et al. (1993).

Here we present a thorough characterization of the diagenetic evolution of clay minerals in the Rotliegend sandstone reservoir of the Broad Fourteens basin (Dutch sector, Southern North Sea) and determines the sequence of diagenetic reactions affecting several blocks with contrasting burial histories. We also describe the structural modifications affecting clay minerals (both kaolin-group and illitic minerals) by numerical processing of the XRD profiles recorded on oriented preparations, by XRD on randomly oriented specimens, and by differential thermal analysis (DTA). Additional K/Ar dating and chemical considerations allow further constraints to be placed on the absolute timing of diagenetic events and on the nature of the fluids responsible for clay-mineral crystallization, respectively.

GEOLOGICAL SETTING

The Lower Permian Rotliegend reservoir is the most important gas reservoir of the southern Permian gas province, which extends from the British sector of the Southern North Sea to Poland (Gaupp et al. 1993). Rotliegend deposition took place in an arid continental basin with areas of eolian dunes, wet interdunes, and alluvial-fan sequences (Glennie 1972). The Rotliegend reservoir is 200–300 m thick and is sealed vertically and laterally (locally) by Upper Permian Zechstein evaporites. Rotliegend sandstones show a marked variability in depositional texture and mineralogy from facies to facies. Within the study area, stratified eolian sandstones are usually well sorted with rounded grains; they range from quartz arenites to sublithic arenites. Wet interdune facies consist of fine to medium, poorly sorted argillaceous sandstones. Fluvial sandstones are poorly to moderately sorted and range from sublithic arenite to conglomerate. The petrophysical parameters of the Rotliegend reservoir show a marked variability, which is strongly influenced by the combined effect of primary sedimentology and subsequent diagenetic history (Seeman 1982).

The study area, known as Broad Fourteens Basin (BFB), is in the Dutch sector of the southern North Sea (Fig. 1). It lies in a graben trending N30–40°W whose subsidence began during Permian time and reached maximal burial depth during the Late Jurassic. In the BFB, the Rotliegend sequence lies unconformably upon Carboniferous source rocks (Westphalian Coal Measures). In the central part of the graben, the sedimentary pile may be almost complete (from Carboniferous to Quaternary), whereas the margins of the basin have been buried much less deeply because of a lower sedimentation rate and repeated deposition and erosion cycles (van Wijhe 1987). The major part of the BFB has been deeply eroded during a complex tectonic history that, after general subsidence from Permian to Middle Jurassic, began with the regional uplift and the increased heat flow of the Kimmerian orogenic phase related to the opening of the Atlantic Ocean (~ 155 Ma) and was followed by two other tectonic disturbances during Cretaceous and Tertiary time (Lee et al. 1989). As a consequence of this complex structural history, the Permian North Sea basin was broken into numerous fault blocks, each with a unique burial history. In the BFB, the Lower Permian formations show dramatic differences in present burial depth (from 2500 m to 4500 m) over relatively short distances. Additionally, these present depths are usually less than maximum burial depths attained before the Kimmerian uplift over the whole BFB area (van Wijhe 1987). From vitrinite reflectance and sonic velocity data, differences between maximum and present burial depths reach 1500–2000 m in the middle part of the basin (Petroland, internal report). Throughout the paper, estimated maximum burial depth is used as an indicator of diagenetic conditions, because of its objectivity. However, burial temperature is related to the maximum burial depth parameter; it increases regularly with burial depth from deposition time (~ 275 Ma) to the Kimmerian orogeny (~ 155 Ma). Additionally, during the Kimmerian orogeny increased heat flow raised temperature to its maximum, ranging from ~ 110°C (3000 m) to ~ 165°C (5000 m), in agreement with fluid-inclusion data (Petroland, internal report).

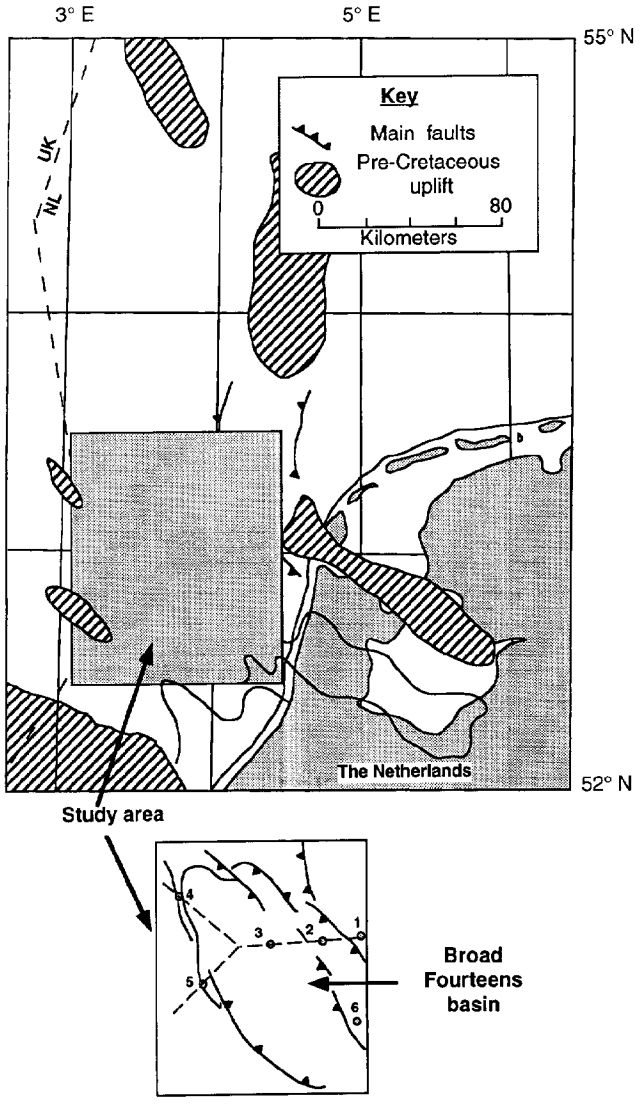

FIG. 1.—Location map of the Broad Fourteens Basin structure in Southern North Sea. The location of the six wells studied (circles labeled 1–6) is shown relative to the graben structure.

Diagenesis of Rotliegend sandstones has been studied all over the southern North Sea and northern Europe (Rossel 1982; Seeman 1982; Pye and Krinsley 1986; Goodchild and Whitaker 1986; Lee et al. 1989; Bjørlykke and Aagaard 1992; Platt 1993; Gaupp et al. 1993). Even though the nature of the authigenic minerals is relatively simple (quartz overgrowths, carbonate and sulfate cements, and clay minerals in which kaolinite and/or illitic minerals predominate), the diagenetic histories proposed by the various authors remain rather controversial. There are strong divergences on the timing of mineral authigenesis; on the basis of petrographic or textural parameters, several crystallization stages are usually suggested, even on a very local scale. Similarly for clay minerals, several generations of illitic minerals and/or kaolinite, related to the major tectonic episodes, are usually invoked, with major implications for reservoir geochemistry and hydrology (e.g., flushing of meteoric water).

TABLE 1.—*Present burial depth and estimated maximum burial depth (see text) for the six wells studied*

Well	Samples Collected	Present Depth (m)	Estimated Maximum Burial Depth (m below sea floor)
1	13	2975–2990	3000
2	12	3320–3495	3300–3500
3	19	4230–4503	3200–4500
4	14	2480–2546	4500
5	13	2880–2970	5000
6	14	2893–2932	3500

SAMPLES AND METHODS

Samples.—The core samples of Rotliegend sandstone reservoir we studied (Table 1) were collected from six wells, five of which are roughly distributed along a cross section of the Dutch part of the BFB (Fig. 1). The sedimentary facies, and consequently the initial mineralogy, of the six wells are fairly homogeneous (eolian sandstones). The estimated paleo-burial depths and the temperatures experienced by the Rotliegend sandstones in these wells before Kimmerian uplift increase from east (~ 3000 m; Well 1) to west (~ 5000 m; Well 5). Authigenic clay minerals are mostly kaolin and illitic minerals. The sixth well was sampled in the southern part of the BFB from a zone in which kaolinite is absent.

Sample Preparation.—Samples were gently crushed to obtain grains about 2 mm in diameter. Rock fragments were then shaken mechanically in water for 12 hr to extract as much clay-size material as possible. Next, remaining rock fragments and coarser grains (approximately > 50 μm) were removed by sedimentation, and the suspension was ultrasonically dispersed. The < 5.0 μm size fractions were obtained by sedimentation (upper 2 cm of the suspension after settling for 15 minutes). When larger quantities of material were required, as for K/Ar dating or XRD on randomly oriented preparations, size fractionation was performed as follows. (1) From a < 20.0 μm fraction, the < 1.0 μm fraction was thoroughly extracted by successive dispersion and sedimentation cycles, the > 1.0 μm being collected as < 20.0 μm fraction. (2) With successive dispersion and centrifugation cycles, the < 0.2 μm fraction was extracted first from the < 1.0 μm size fraction. (3) The 0.2–0.5 μm fraction was extracted in a second series of dispersion and centrifugation cycles. (4) The remaining fraction (0.5–1.0 μm) was collected. No cation exchange was performed. This is assumed to have little influence on peak position, because the I/S are highly illitic. Lanson and Besson (1992) showed on samples with very similar clay parageneses that Sr saturation does not significantly modify I/S peak position. Furthermore, Lanson (1990) showed theoretically that the presence of up to 25% smectite layers saturated with one water layer does not greatly influence peak position for such highly illitic I/S (> 90% illite). Oriented slides were prepared by drying a few milliliters of the suspension on an aluminum slide. High-gradient magnetic separation (Righi and Jadault 1988) was performed using a 0.5 T magnetic field on a few samples to separate part of the detrital mica from well crystallized authigenic illite.

For SEM observations, freshly fractured rock fragments were gold-coated. SEM observations were made on either a JEOL-35C or a JEOL-6400, both equipped with an energy dispersive spectrometer.

DTA analyses (thermogravimetry; TGA) were performed on the < 20.0 μm size fraction because of the greater abundance of kaolin-group minerals (see below). Analyses were performed on a Netzsch STA 409 EP, heating a 20 mg sample up to 1100°C at 10°C/minute.

Size fractionation for K/Ar dating was performed as described above; sample mineralogy was checked by XRD both on oriented clay slides and on randomly oriented preparations. Argon was measured using a mass spectrometer calibrated for ^{38}Ar and corrected for ^{36}Ar. K was measured using a flame spectrometer, or using the isotope dilution method if the K content was too low.

TABLE 2.—*Experimental conditions used for X-ray diffraction data collection*

Type of Preparation	Angular Range °2θ CuKα	Scanned Range Å	Step Size °2θ CuKα	Counting Time Seconds
Randomly oriented preparations (bulk rock)	2–70	44.0–1.35	0.02	1.0
Randomly oriented preparations (clay separates)	2–70 19–36	44.0–1.35 4.65–2.50	0.01–0.02	6.0–12.0
Oriented slides (clay separates—air-dried state)	2–33	44.0–2.7	0.02	1.2
Oriented slides (clay separates—glycerol solvated)	2–23	44.0–3.9	0.02	1.2
Oriented slides for decomposition (clay separates—air-dried state)	2–14 14–33	44.0–6.3 6.3–2.7	0.01 0.025	5.0 5.0
Oriented slides for decomposition (clay separates—glycerol solvated)	2–23	44.0–3.9	0.02	5.0

X-Ray Diffraction.—All samples were run on a Philips PW1729 diffractometer equipped with a stepping-motor drive on the goniometer, and a sample spinner. Motor and intensity acquisition commands were effected using a Socabim DACO system. Diffracted-beam-monochromated Cu $K_{\alpha 1+2}$ radiation was used (30 kV, 50 mA). Divergence slit, receiving slit, and scatter slit were 1°, 0.1 mm, and 1°, respectively. Variable slits were used to run oriented slides of clay separates. Glycerol solvation was performed using liquid glycerol as a spray. Relative humidity was not controlled during data collection. Experimental conditions used for XRD data collection are detailed in Table 2.

XRD Profile Interpretation.—Phase identification with XRD is commonly performed by comparison with simulated profiles, but the trial-and-error method is so time-consuming that various alternative methods have been proposed for "quick" identification of clay minerals and especially of I/S (Środoń 1979, 1980, 1981, 1984b; Watanabe 1981, 1988; Velde et al. 1986). However, these methods are difficult to apply routinely, either because they require measurements on low-intensity higher-angle peaks or because they necessitate separation of diffraction effects from the various clay phases coexisting in the sample (Lanson and Besson 1992). Usually these phases are characterized globally with the Kubler index (Kubler 1964, 1968), and no detail can be obtained on individual populations (e.g., I/S and illite relative proportions, I/S composition, illite crystallinity). To take into account the simultaneous presence of several phases (I/S mixed-layered phases) with closely related crystallographic characteristics resulting from illitization kinetics (Lanson and Velde 1992), XRD profiles must be processed numerically. XRD profile decomposition allows accurate characterization of these coexisting phases and of their respective evolutions (Lanson and Besson 1992; Lanson and Velde 1992). We used the DECOMPXR program (Lanson and Champion 1991; Lanson and Velde 1992) on our samples to show changes in I/S composition (i.e., illite content) by determining the I/S peak position (Fig. 2). Decomposition was performed routinely on the 5–11° 2θ (17.6–8.0 Å) range of the air-dried (AD) profile. However, as suggested by Lanson and Velde (1992), identification of the various populations of illitic particles (I/S, poorly crystallized illite, well crystallized illite) performed on this limited range was checked, for some samples, against data available from other diffraction bands of the AD profile. Additionally, special attention was paid to obtain consistent results also from the decomposition of both AD and glycerol-solvated (GLY) profiles of the same sample (Fig. 2).

Further, with XRD profile decomposition it is also possible to follow both (1) the change in relative proportions of I/S and illite (*sensu stricto*) by using intensity ratios between I/S and both illite peaks and (2) the evolution of illite (*sensu stricto*) crystallinity (i.e., mean coherent scattering domain size; CSDS). Lanson et al. (1995) developed a new crystallinity index to take into account both the relative proportions of poorly and well crystallized illite peaks (PCI and WCI, respectively) and the mean CSDS

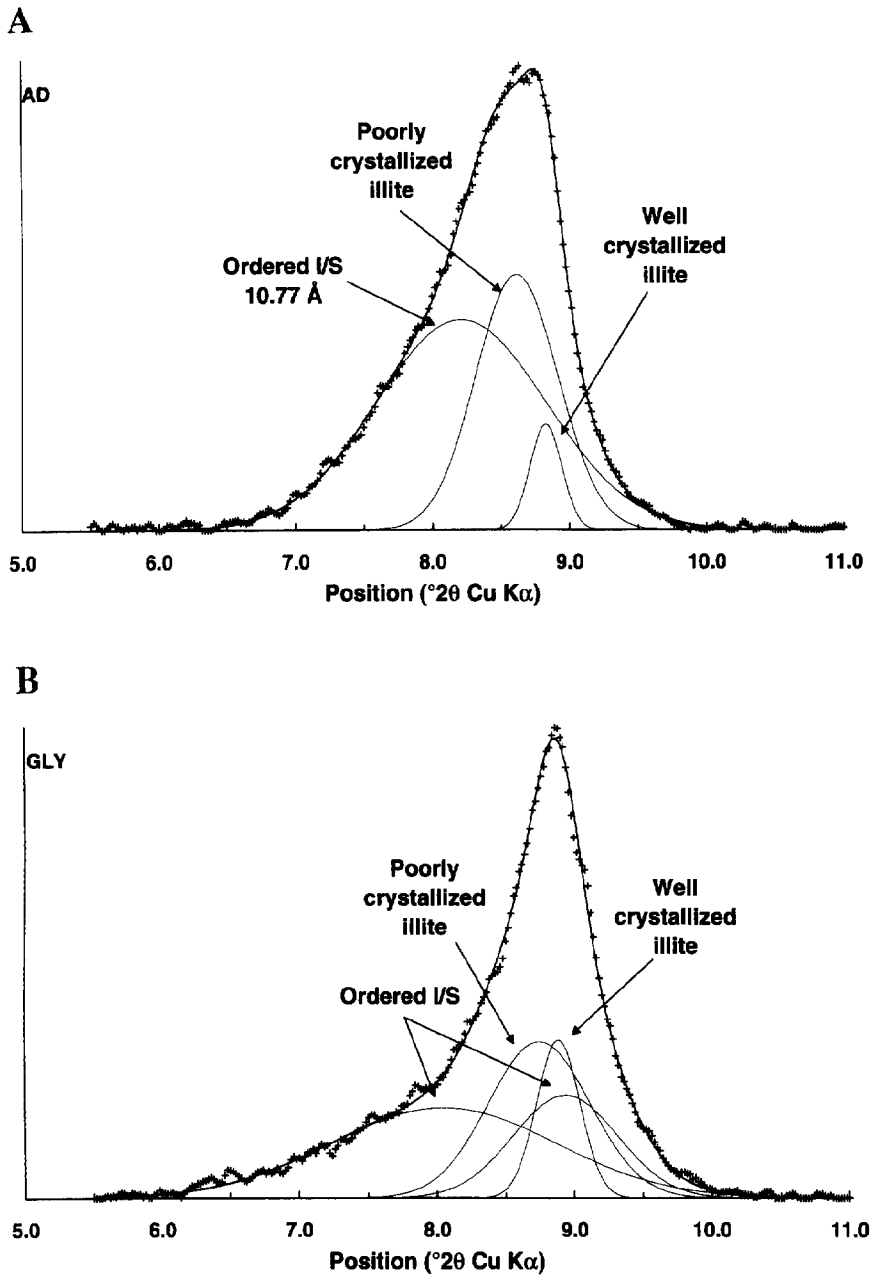

FIG. 2.—Decomposition of both **A)** air dried (AD) and **B)** glycerol solvated (GLY) XRD profiles of sample Well 2, 3321 m. For decomposition of the GLY profile there should be an elementary peak associated with any elementary peak fitted on the AD profile (Lanson and Besson 1992). Furthermore, if this elementary peak is associated with an expandable I/S phase, an additional peak must be introduced, because a doublet is associated with glycerol-solvated I/S mixed-layer phases in this angular range (one peak on each side of 10.0 Å).

of the poorly crystallized population (which influences both the PCI peak position and its full width at half maximum intensity; FWHM):

$$\text{Crystallinity} = \frac{0.1}{\%\text{Int}_{\text{PCI}} \cdot \text{FWHM}_{\text{PCI}} \cdot (\text{Pos}_{\text{PCI}} - \text{Pos}_{\text{WCI}})}.$$

Relative intensity of the PCI peak, i.e., PCI int./(PCI int. + WCI int. + I/S int.), is expressed in percent, and peak positions are expressed in Å, whereas peak FWHM is expressed in °2θ Cu K_α. When illite is better crystallized, this index increases, as the CSDS, whereas the Kubler index decreases. Differentiation between PCI and WCI is simply a convenient way to describe the illite population; it does not imply the actual existence of two distinct populations of illite particles (Lanson and Meunier 1995).

Characterization of the polytype and of the distribution of the cations between, for example, the *cis* and *trans* octahedral sites is based on comparison with computer-simulated XRD profiles (Drits et al. 1990; Reynolds 1993). According to Drits et al. (1993), diagnostic peaks (Fig. 3, Table 3) are located in the 19–34° 2θ range (4.65–2.65 Å). The characterization of kaolin-group minerals was performed on the 19–26° 2θ (4.65–3.45 Å) range (Fig. 4, Table 4) using XRD data of Bailey (1980). Additionally, (11-1) and (02-1) kaolinite peaks were used to estimate structural disorder in kaolinites (Drits et al. 1990).

EXPERIMENTAL RESULTS

Petrology

Diagenetic Sequence.—In Rotliegend deposits, dissolution of detrital minerals (mostly feldspars) and pore filling by authigenic minerals (car-

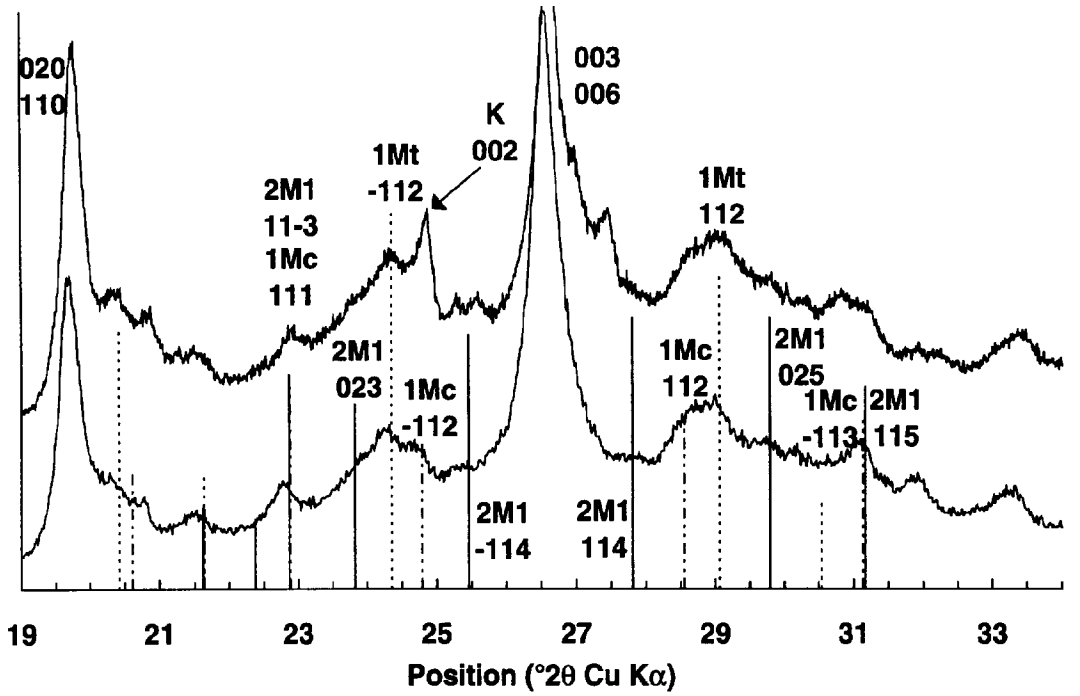

FIG. 3.—Diagnostic lines for illite polytype identification. *d* values and relative intensities for the various polytypes have been calculated by Drits et al. (1993). Solid line, $2M_1$ polytype; regular dashed line, 1M with octahedral *trans* sites vacant (1Mt) polytype; irregular dashed line, 1M with octahedral *cis* sites vacant (1Mc) polytype. Experimental XRD patterns are from the 0.5–1.0 μm size fraction of samples Well 2, 3350 m (top) and Well 3, 4248 m (bottom).

bonates, quartz, kaolin, illitic minerals, sulfates) indicate a diagenetic sequence similar to that described by Rossel (1982) for clay minerals and by Pye and Krinsley (1986) for carbonates and evaporite minerals. The general sequence can be summarized as follows:

(1) Early crystallization of carbonates (mostly siderite) and possibly sulfates.

(2) Progressive infilling of primary pores by euhedral carbonates (ferroan dolomite to ankerite), quartz overgrowths, and kaolin aggregates. Numerous features of intergrowth (i.e., mutual stopping of faces) between these three phases may be observed (Fig. 5A, B). Dissolution of both plagioclase and K-feldspar is clearly concomitant with the crystallization of euhedral carbonates, kaolin, and quartz, as deduced from petrographic observations (mutual stopping of carbonates, kaolin and quartz growth faces), as well as from XRD data (inverse evolution of the relative proportions of carbonates, quartz, and kaolin on the one hand, and of plagioclase and K-feldspar on the other hand).

TABLE 3.—*Positions and Miller indices for X-ray diffraction lines characteristic of illite 1M with octahedral trans sites vacant (1Mt), 1M with octahedral* cis *sites vacant (1Mc), and $2M_1$ polytypes (from Drits et al. 1993)*

1Mt		1Mc		$2M_1$		
Pos. (Å)	hkl	Pos. (Å)	hkl	Pos. (Å)	hkl	Remark
3.655	−112	3.591	−112			Peak shift is characteristic of 1Mt-1Mc illite polytypes
3.073	112	3.126	112			Peak shift is characteristic of 1Mt-1Mc illite polytypes
		3.885	111	3.889	11-3	Line common to 2M1 and 1Mc polytypes
		2.873	−113	2.870	115	Line common to 2M1 and 1Mc polytypes
				3.735	023	Characteristic line for 2M1
				3.500	−114	Characteristic line for 2M1
				3.208	114	Characteristic line for 2M1
				2.999	025	Characteristic line for 2M1

(3) Illitization at the expense of kaolin aggregates (Fig. 5C, D). Most often, hematite is associated with illitic minerals.

(4) Late crystallization of sulfates (anhydrite and barite) and less commonly siderite. These cements postdate illitization and locally seal both primary and secondary porosity. These minerals are especially abundant close to the Zechstein evaporitic cap, which overlies the Rotliegend sandstones reservoir.

Variations in Diagenetic Sequence of Non-Clay Minerals.—Except for relative proportions and abundances of kaolin-group and illite-group minerals, which are described extensively below, diagenetic features observed in the six wells are fairly uniform, with three exceptions. (1) There are slight changes in the nature of authigenic non-clay minerals, e.g., the local presence of authigenic albite, late siderite, or traces of carnallite. (2) Textural changes such as progressive increase in average grain size occur with increasing paleo-burial depth. (3) There is a clear increase in dissolution of detrital K-feldspar and plagioclase with burial depth. At shallower burial depth (3000 m; Well 1), K-feldspar is common and only partly dissolved, whereas no K-feldspar relics remain below the burial depth of 4000 m. Although very altered, plagioclase is still present in Well 1 (3000 m) and at the top of Well 2 (3300 m); no plagioclase is observed below a burial depth of 3400 m.

Kaolin-Group Minerals

Petrography and Morphology.—Kaolin was observed in the five wells of the middle part of the BFB (Wells 1 to 5) in relative proportions varying from 1% to 15%. This large variation is related neither to the well location nor to estimated maximum burial depth or temperature. Kaolin is absent in the Rotliegend sandstones of the well in the southern part of the BFB, which contains significant proportions (up to 5% in volume) of detrital K-feldspars and is strongly illitized. Kaolin is developed mostly as pore-filling aggregates of coarse-grained crystals, and occasionally as isolated crystals scattered on detrital quartz grains.

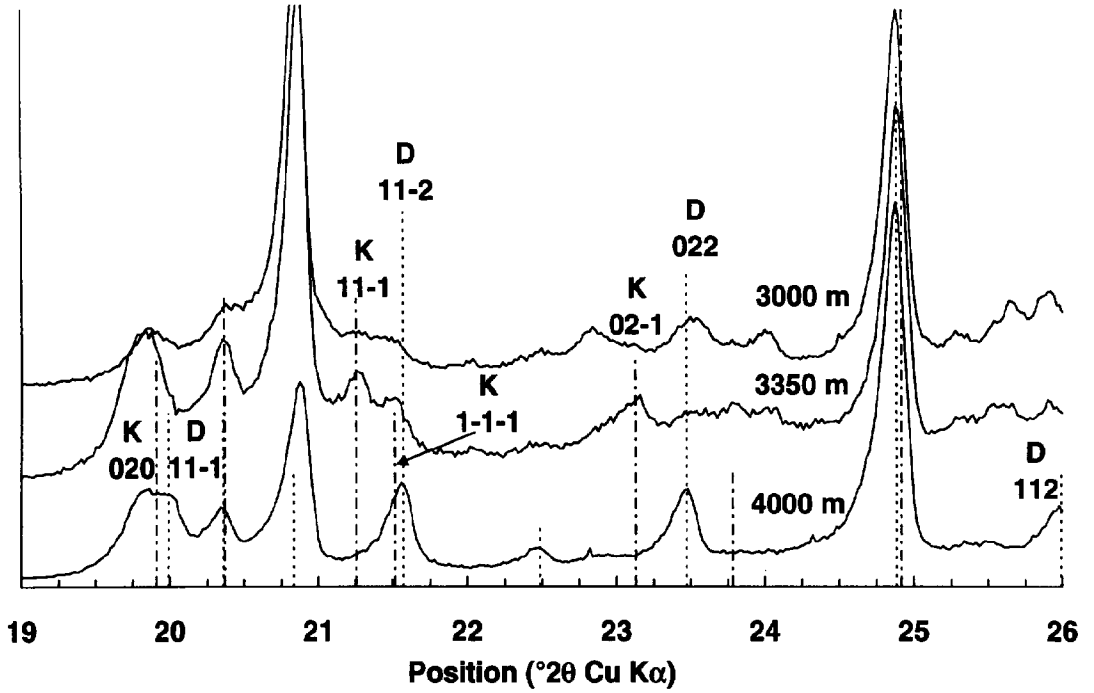

FIG. 4.—Diagnostic lines for kaolin-group mineral identification. *d* values and relative intensities are from Bailey (1980). Regular dashed line, dickite; irregular dashed line, kaolinite. Experimental XRD patterns are from the 1.0–20.0 μm size fraction of samples Well 1, 2976 m (top), Well 2, 3358 m (middle), and Well 3, 4248 m (bottom).

Where present, kaolin shows regular changes in morphology with increasing maximum burial depth. In the well with the shallowest burial (estimated to be 3000 m, ~ 110°C), kaolin shows vermicular habits typical of kaolinite (Fig. 6A); the average diameter of kaolinite books is < 10 μm. Intergrowths of larger (diameter > 10 μm) blocky crystals (dickite) are in some places observed within the pore-filling vermicules of kaolinite. The thickness (along the *c** axis) of hexagonal kaolinite books increases regularly with depth (~ 1 μm around 3500 m; Fig. 6B), and the average diameter of these mixed kaolin books increases to 20 μm around 3500 m (Lanson et al. 1995). Further, crystals with dickite morphology can be clearly seen in the stacking sequence of thin euhedral plates (Fig. 6B). At an estimated burial depth of 4000 m, the number of kaolin crystals stacked on top of each other strongly decreases. Stacks of a few dickite crystals totally replace kaolinite book structures. In wells with deeper burial (4500 m), dickite pseudomorphs of kaolinite books are no longer observed; all the kaolin is formed by aggregates of individual coarse-grained isometric dickite crystals whose diameter may be larger than 25 μm (Fig. 6C). In Well 2, this conversion occurs over a depth interval of only 300 m from top to bottom of the Rotliegend sandstone reservoir.

TABLE 4.—*Positions and Miller indices for X-ray diffraction lines characteristic of kaolinite and dickite (from Bailey 1980)*

Kaolinite		Dickite		
Position (Å)	*hkl*	Position (Å)	*hkl*	Remark
4.46	020	4.439	11-1	Peak shift indicates the presence of kaolin polytypes
4.18	11-1			Structural disorder in kaolinite
4.13	1-1-1	4.119	11-2	Peak shift indicates the presence of kaolin polytypes
		3.790	022	Additional dickite line
		3.428	112	Additional dickite line
3.845	02-1			Structural disorder in kaolinite

All kaolin-group minerals, whatever their polytype, were subjected to dissolution during subsequent illitization. Dissolution of the kaolins is closely related to illitization intensity in the various wells. Typically, partly dissolved books of kaolinite show ragged or rounded edges (Lanson et al. 1995), whereas partly dissolved blocky crystals of dickite show smoothed shapes without preferential direction of etching (Fig. 6D).

X-Ray Diffraction.—The steady evolution of kaolinite to dickite with increasing estimated maximum burial depth is clearly shown in Figure 7. The shallowest samples contain mostly poorly crystallized kaolinite (very weak 11-1 and 02-1 kaolinite peaks). Then, within a rather narrow range of burial depth (3350–3450 m, Well 2) improvement in kaolinite crystallinity is manifested by increased intensity of kaolinite 11-1 and 02-1 peaks. At the bottom of Well 2 (~ 3500 m) the transition between this well-crystallized kaolinite and dickite is achieved, and only dickite can be identified in deeper samples. The polytype modification occurs prior to the major change in morphology, i.e., the evolution from thick booklets to blocky crystals.

Differential Thermal Analysis.—The progressive character of the kaolinite-to-dickite transition is also clearly shown using DTA (Fig. 8). The 0.5–1.0 μm fraction of sample from 2976 m in Well 1 has a dehydroxylation temperature profile characteristic of kaolinite (Mackenzie 1970). On the contrary, the well crystallized kaolinite, which is present in a more deeply buried sample (3350 m, Well 2), has a broadened dehydroxylation temperature peak that is clearly shifted towards higher temperatures, i.e., towards the dehydroxylation temperature of dickite. In addition to the dehydroxylation peak characteristic of dickite, such a broad shifted peak is observed also in the DTA profile of sample from 4285 m in Well 3 even though this sample contains exclusively dickite (see above).

Illitic Minerals

Petrography and Morphology.—The petrography of illitic material in the BFB is very similar to what has been reported previously for the Rotliegend sandstones reservoir in other areas (Rossel 1982; Goodchild and

FIG. 5.—**A)** Sample from Well 1 (2988 m). Simultaneous growth of kaolinite books and quartz inducing intergrowth features. Additional presence of authigenic ankerite. **B)** Sample from Well 4 (2479 m). Simultaneous crystallization of dickite and quartz, showing mutual stopping of growth faces. **C)** Sample from Well 3 (4285 m). Illite crystallization on kaolin growth sites (see **A** and **B**) at the surface of a quartz crystal. **D)** Sample from Well 2 (3492 m). Illitization of kaolin aggregates.

Whitaker 1986; Pye and Krinsley 1986; Lee et al. 1989; Platt 1993; Gaupp et al. 1993). Illitic minerals typically are present either as aggregates of monocrystalline euhedral crystals as replacements of pore-filling kaolin aggregates (Fig. 5D) or as coatings 5–15 μm thick on the surfaces of the framework quartz grains (pore-lining; Fig. 9A). In wells showing intense illitization of Rotliegend sandstones, these coatings are often two-layered, with a compact inner layer and an outer layer composed of laths growing radially into the pores and filling intergranular voids (pore-bridging; Fig. 9A, B). Additionally, authigenic illitic minerals commonly grow on the surface of secondary quartz grains and Mg- and Fe-carbonates and as replacement of kaolin (Fig. 5C).

The shape and size of illitic-mineral euhedral crystals vary significantly with estimated maximum burial depth. In the shallowest well (3000 m), illitic crystals are very elongated, filamentous, almost one-dimensional particles (whiskers; Fig. 9B). The maximum width of these hairy illitic particles reaches 0.3–0.5 μm. With increasing paleo-burial depth, illitic minerals show first a more rigid lath morphology (Fig. 9C). These lath-shaped crystals are assumed to be elongated along their *a* axis (Rex 1965; McHardy et al. 1982); their maximum width is about 2.0 μm at 3500 m (Lanson et al. 1995), and reaches 3.0–5.0 μm below 4000 m. Crystal coarsening of illitic minerals with increasing depth is associated with a morphological evolution. Even though lath-shaped particles make up the dominant population of illitic minerals throughout the six wells studied, whatever their estimated maximum burial depth, isometric pseudo-hexagonal-shaped particles are present from 4000 m and deeper (Fig. 9D); the proportion of these isometric plates increases with depth. Their maximum diameter attains 3.0–5.0 μm around 4500 m (Lanson et al. 1995). This morphological evolution is related to the modification of the 3-D structure of illitic minerals with increasing paleo-burial conditions.

Finally, even though crystal size and morphology are related to maximum paleo-burial depth in the six wells studied, the intensity of illitization (abundance of illitic minerals in the clay-size fraction) of the Rotliegend reservoir varies from one well to another independently of depth. For example, relative intensities of illitic minerals and kaolinite peaks on XRD diagrams (Fig. 10) and SEM observations indicate that dissolution of kaolin and illitization are intense in Well 5, whereas in Well 4 kaolins are only slightly altered and illitization is weak and not pervasive, in spite of the very similar burial histories of the two wells.

X-Ray Diffraction.—In diffractograms of oriented preparations (both AD and GLY) from the Rotliegend reservoir clay separates (Fig. 10) one can

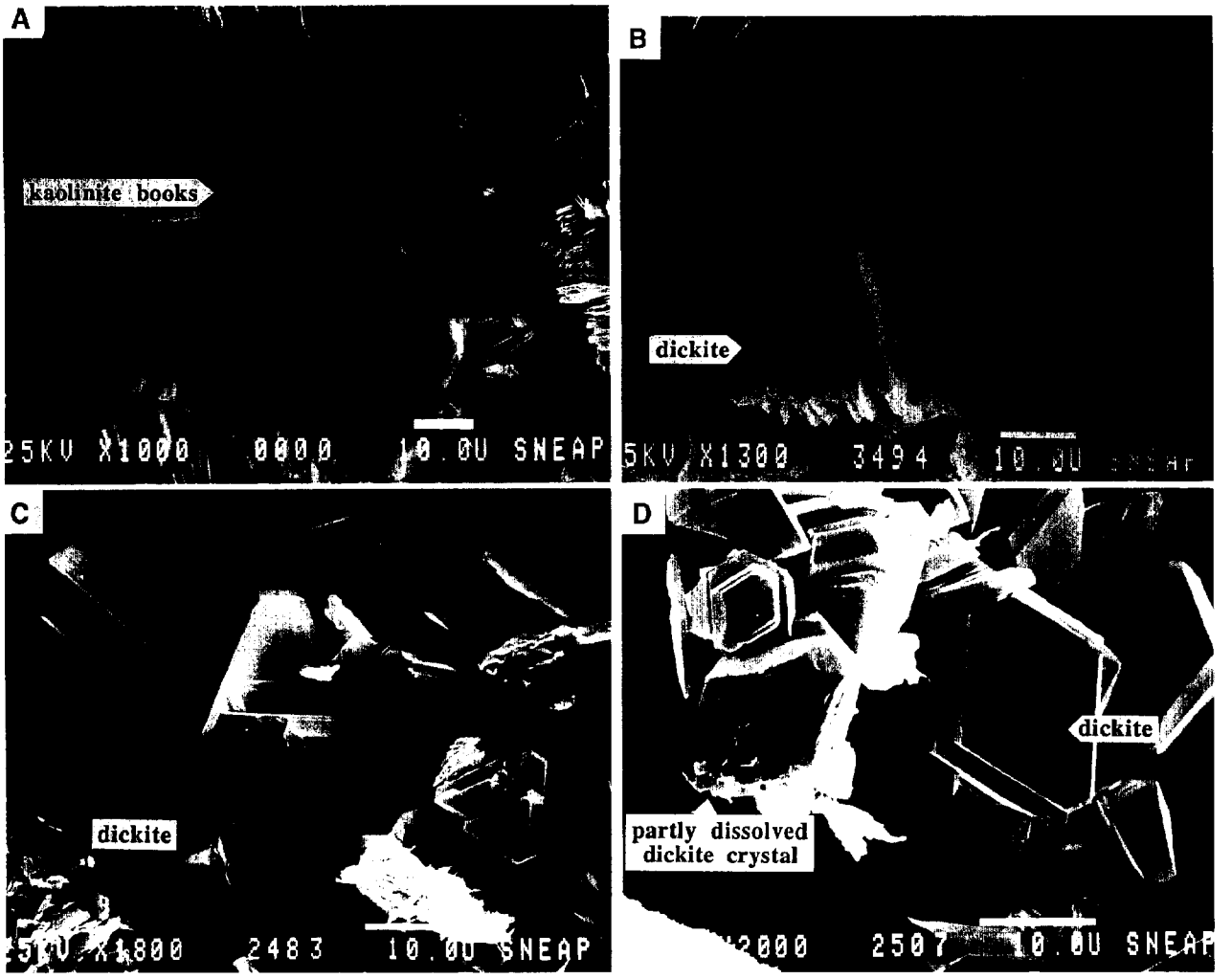

FIG. 6.—**A)** Sample from Well 1 (2976 m). Kaolin-group minerals exhibit vermicular habits typical of kaolinite (books). **B)** Sample from Well 2 (3494 m). Stacks of a few thick dickite crystallites replace kaolinite books. **C)** Sample from Well 4 (2484 m). Coarse isometric dickite crystals. Note the dramatic change in the morphology of dickite. **D)** Sample from Well 4 (2507 m). Among unaltered dickite crystals, partly dissolved blocky crystal of dickite has smoothed shapes without preferential direction of etching.

observe the classic increase of illite "crystallinity" (decreasing width of the 10.0 Å band) with increasing burial depth. This increase results both from illite growth on both illite and I/S particles and from crystallization of illite at the expense of illitic I/S. The decomposition treatment (Fig. 11) allows one to separate the contributions of the various effects on peak shape. In Figure 11, one can note visually both the decrease in I/S peak relative intensity, related to illite crystallization at the expense of illitic I/S, and shift of the I/S peak towards 10.0 Å, related to illite growth on I/S particles. Furthermore, relative intensities of poorly and well-crystallized illite peaks vary with estimated maximum burial depth. The well crystallized micaceous phase was identified as authigenic illite except for the shallower sample (Well 1, 2976 m), in which detrital mica has been observed. Most of this detrital contribution is removed with high-gradient magnetic separation (nonmagnetic fraction), whereas for more deeply buried samples such a treatment does not modify the relative intensities of poorly and well crystallized illite peaks. Consequently, only poorly crystallized authigenic illite is present in the shallower sample; with increasing maximum burial depth, the relative contribution of WCI increases, and the PCI peak position shifts towards 10.0 Å and becomes sharper, to indicate an increasing mean CSDS. From the decomposition procedure, these changes can be quantified accurately (Figs. 12A–C). Figures 12A–C show that any of these parameters, i.e., I/S peak intensity ratio (I/S relative abundance), I/S peak position (illite content of I/S), and illite crystallinity (illite mean CSDS), evolves steadily with increasing burial depth and is characteristic of the maximum burial depth reached by the Rotliegend sandstone reservoir.

In addition to this evolution of the illite/smectite stacking sequences (thickness of the stacking sequences, as well as relative proportions of both end members) along the c^* axis, the 3-D crystallochemical structure of these illitic minerals evolves with burial depth (Fig. 13) from 1M with octahedral *trans* sites vacant (1Mt) to 1M with octahedral *cis* sites vacant (1Mc). Relative intensities of their respective -112 and 112 XRD peaks show that 1Mt is the prevailing polytype in shallower samples, whereas the proportion of 1Mc polytype increases with burial depth as indicated also by the increased intensity of 1Mc XRD peaks (e.g., 111, -113). This polytype evolution occurs even for small differences in burial depth (e.g., from top to bottom of Well 2; Fig. 13). Furthermore, the proportions of 1Mc polytype also increase with the size fraction (Fig. 14).

K/Ar Geochronology.—The problem of contamination by detrital illite is

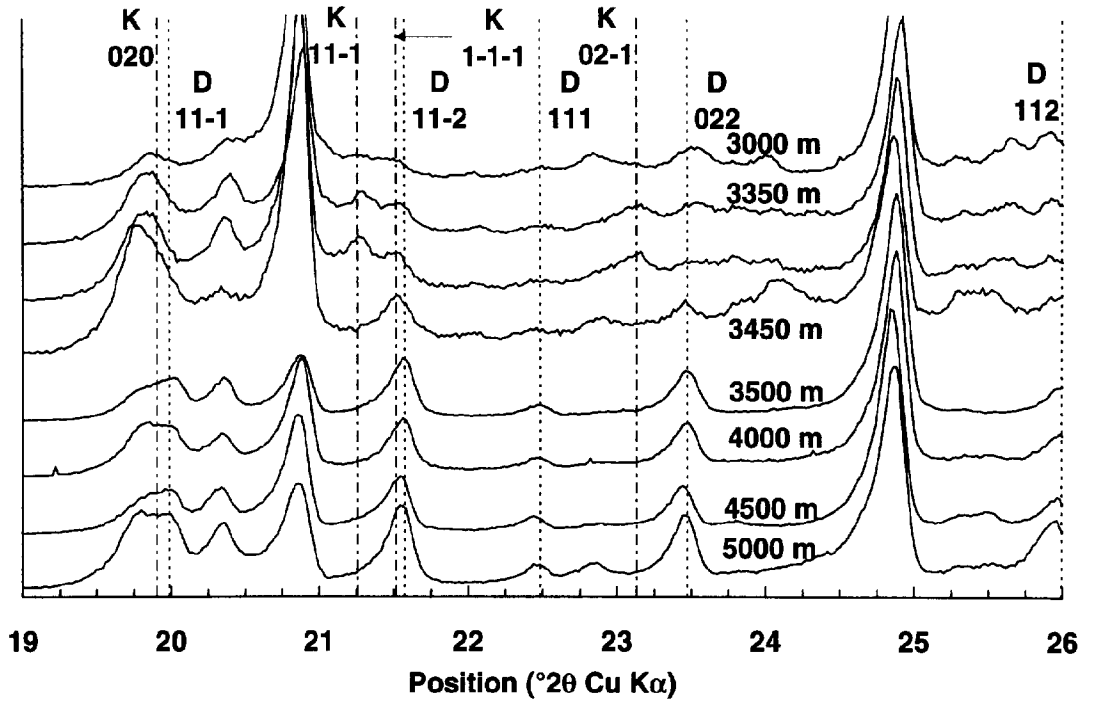

FIG. 7.—Evolution of the 3-D crystallographic structure of kaolin-group minerals as a function of estimated maximum burial depth. From top to bottom: 1.0–20.0 μm fractions of samples from Well 1 (2976 m), Well 2 (3350 m, 3358 m, 3445 m, and 3495 m), Well 3 (4248 m), Well 4 (2545 m), and Well 5 (2968 m). Patterns for kaolinite (Dry Branch) and dickite (St. Claire, PA) reference samples are same as in Figure 4.

minimized by the eolian origin of the samples studied (Lee et al. 1989). Contamination and dilution by other phases was checked by XRD, and minimal dilution by non-K-bearing phases is supported by the fairly high K contents (pure illite contains 8.8% K). Except for the coarser size fractions of samples from Well 1, where detrital mica is present and authigenic illite is rare (kaolinite dominant; very low K content) and for samples from Well 4, where illite abundance is low (both series of samples are shown in gray in Figure 15), the K/Ar ages obtained on the various size fractions from the six wells are fairly consistently between 145 Ma and 165 Ma and were not differentiated (Fig. 15; mean value 157 Ma). These values coincide with the first period of regional tectonic activity (Kimmerian orogeny, ~ 155 Ma).

DISCUSSION

Diagenetic Sequence

From petrographic observations, it appears that precipitation of kaolin and quartz is concomitant with dissolution of both plagioclase and K-feld-

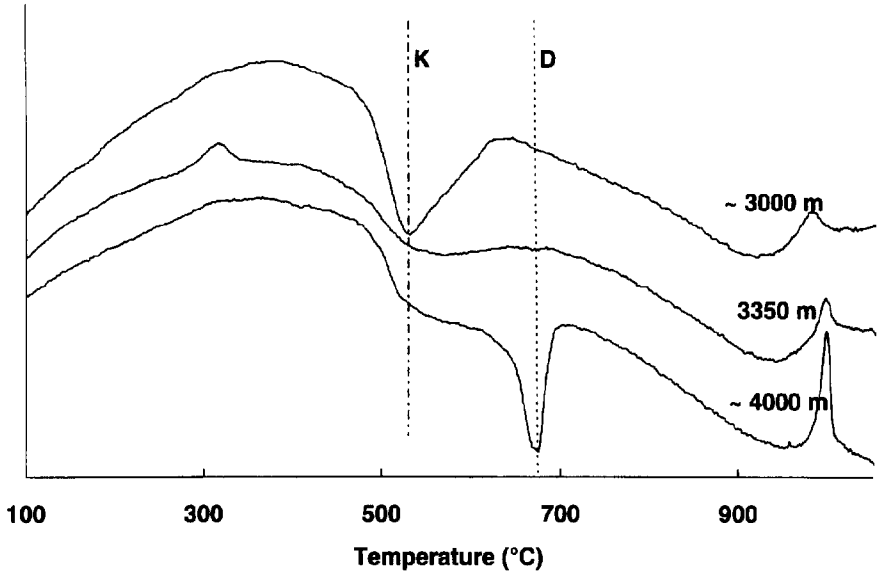

FIG. 8.—Evolution of dehydroxylation temperature as a function of estimated maximum burial depth. From top to bottom: 0.5–1.0 μm fraction of sample from Well 1 (2976 m), 1.0–20.0 μm fraction of samples from Well 2 (3350 m) and Well 3 (4285 m). Patterns for kaolinite and dickite are same as in Figure 4.

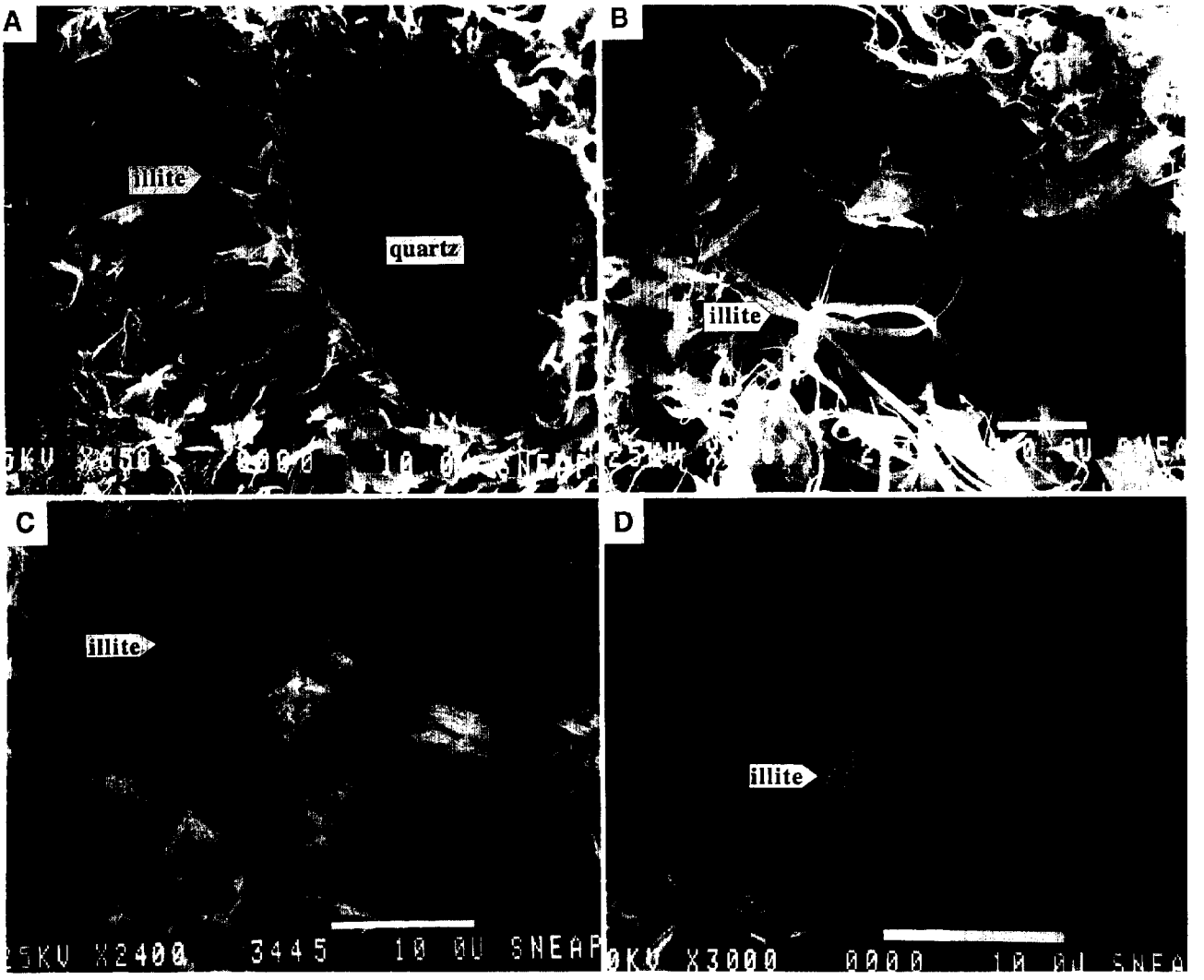

FIG. 9.—**A)** Sample from Well 3 (4341 m). Two-layered coating of illitic minerals growing on a quartz grain and showing a compact inner layer and an outer layer composed of laths growing radially into the pores and filling intergranular voids. **B)** Sample from Well 6 (2947 m). Very elongated filamentous illitic crystals growing radially into the pores (pore bridging). **C)** Sample from Well 2 (3445 m). Lath-shaped particles of illitic minerals. **D)** Sample from Well 3 (4238 m). Isometric pseudo-hexagonal crystals of illitic minerals.

spar; kaolin illitization is superimposed on this early diagenetic transformation and occurs at the expense of kaolin-group minerals subsequent to the kaolinite-to-dickite evolution. However, the morphology as well as the crystallochemical structure of both clay groups recorded the maximum burial depth experienced by the Rotliegend sandstone reservoir. On the one hand, the morphology of kaolin-group minerals steadily evolved from small kaolinite books to larger blocky crystals of dickite with increasing burial depth. On the other hand, fiber- and lath-shaped crystals of I/S and poorly crystallized illite (1M polytype with octahedral *trans* sites vacant) were transformed into more equant, larger, more illitic and better crystallized illite particles (1M polytype with octahedral *cis* sites vacant). From these results several problems arise: (1) the origin and the timing of precipitation of kaolin-group minerals; (2) the driving force of the kaolinite-to-dickite transformation; (3) the driving force inducing kaolin illitization and the timing of this reaction. In the following discussion possible schemes for these mineral reactions are assessed in the light of the thermodynamic calculations and kinetic considerations of Berger et al. (1995).

Origin of Kaolin-Group Minerals

From petrographic evidence, one can assert that kaolin-group minerals in the Rotliegend sandstones reservoir of the BFB result not from a late crystallization episode, as suggested by Goodchild and Whitaker (1986) in the British Rotliegend reservoir, but from early diagenetic reactions. Kaolin-group minerals have formed mostly at the expense of K-feldspars, as observed previously by Rossel (1982) and Pye and Krinsley (1986), and have been subsequently illitized. Hydrolysis of K-feldspars, and subsequent precipitation of kaolinite, is known to consume protons (exchange of H^+ by K^+) through the reaction

$$\text{K-feldspar} + H^+ + 1/2\ H_2O \rightarrow 1/2\ \text{kaolinite} + 2SiO_{2(aq)} + K^+ \quad (1)$$

Reaction (1) is conservative for Al and can be used to define the stability fields of silicates as a function of pH and K^+/H^+ activity ratio in solution. Two diagenetic schemes are usually proposed to account for this reaction: (1) intense leaching by meteoric water; (2) release of protons of organic

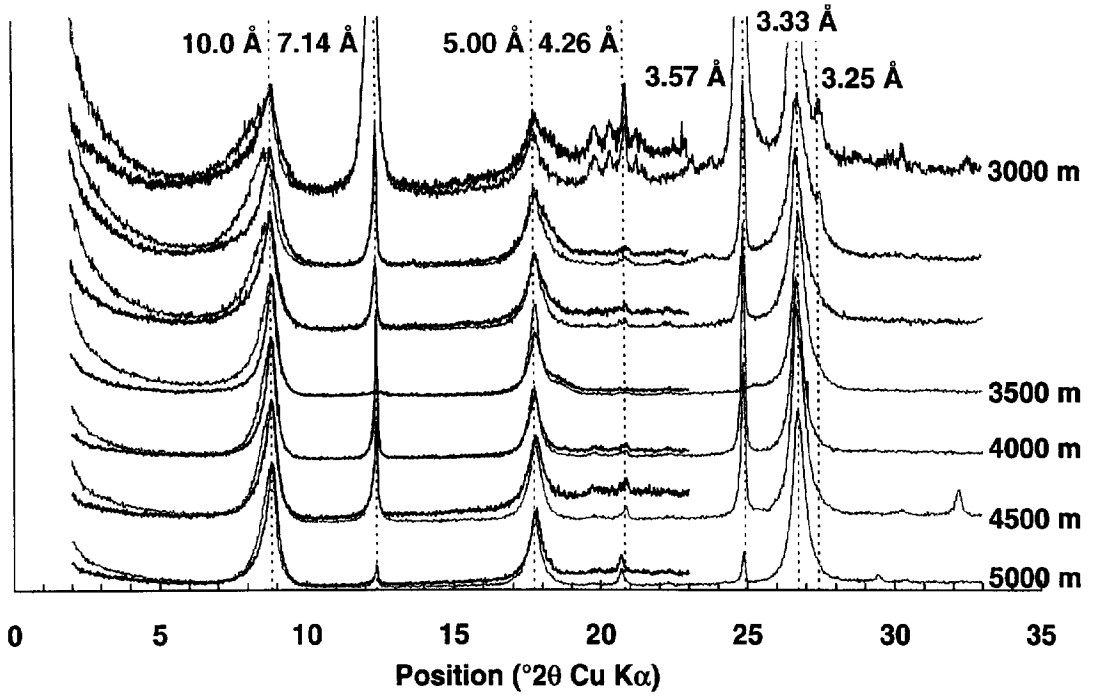

FIG. 10.—Characteristic evolution of clay minerals (< 5.0 μm fraction) as a function of estimated maximum burial depth. Light gray trace, AD profile; black trace, GLY profile. From top to bottom: samples from Well 1 (2976 m), Well 2 (3321 m, and 3445 m), Well 6 (2893 m), Well 3 (4248 m), Well 4 (2545 m), and Well 5 (2968 m). Intensities are normalized on the 10.0 Å peak.

origin in the pore water. The first scheme promotes Reaction (1) if large volumes of water are available, whereas the second scheme, which corresponds to much lower fluid/rock ratios, favors Reaction (1) because of the high acidity of the fluids. In both cases the reaction stops when the K^+/H^+ activity ratio in solution equals the equilibrium ratio for kaolinite. This condition is attained either when all K-feldspar is dissolved or if the K^+/H^+ activity ratio is on the join between the stability fields of K-feldspar and kaolinite.

Platt (1993) indicated from oxygen isotope data that the kaolin-group minerals in the Rotliegend sandstones of northern Germany cannot have grown from meteoric waters. Rather, the conditions of acid formation water required for leaching of feldspars and crystallization of kaolin were believed to have resulted from expulsion of CO_2-enriched waters from the underlying gas-generating Carboniferous Coal Measures (Rossel 1982; Pye and Krinsley 1986). Indeed, organic acids may be released in fluids, because of breakdown at low temperature (peak expulsion at 100°C; Platt 1993) of the kerogen in this formation (Scotchman et al. 1989). Clearly, there is a potential within the Carboniferous Coal Measures sequence for production of large volumes of acidic solutions (Scotchman et al. 1989; Platt 1993). Migration of these solutions into the overlying Rotliegend, evoked by Goodchild and Whitaker (1986), has been clearly shown by Gaupp et al. (1993) and Platt (1993), who demonstrated, in northern Germany, that extensive feldspar dissolution and kaolin growth occur where Rotliegend sandstones are in direct contact (vertical or lateral) with the Carboniferous Coal Measures formation. Additionally, they noted that kaolin may be impregnated with bitumen close to the contact with this formation.

However, when pore water is equilibrated with the K-feldspar/kaolinite/quartz mineral assemblage, muscovite (or end-member illite) is supersaturated whatever the temperature (Bjørlykke and Aagaard 1992). Absence of illite growth, and survival of this metastable assemblage with no limitation on burial depth, can be understood from kinetic considerations (Berger et al. 1995). Berger et al. proposed that the absence of kaolinite-to-illite transformation, which is characteristic of diagenesis in North Sea sandstones, reflects the high energy barrier of this illitization reaction. In contrast to the smectite-to-illite conversion, illitization of kaolinite implies direct precipitation of end-member illite. This precipitation would occur when the system is greatly oversaturated with respect to the end-member illite, and consequently when the system is oversaturated also with respect to K-feldspar. The critical $|\Delta G|_{reaction}$ for illite growth (high oversaturation conditions) cannot be obtained when pore water equilibrates with K-feldspar from undersaturated conditions ("from the bottom"). Consequently, when organic acids are released in the Rotliegend sandstones of the BFB, kaolinite is the dominant authigenic silicate phase.

Furthermore, petrographic data reported by Platt (1993), consistent with the present study, suggest that K-feldspar dissolution cannot be the only source of Al to account for the observed proportion of authigenic kaolinite (up to 15% from point counting on thin sections). Consequently, kaolinite precipitation in Rotliegend sandstones probably resulted also from total (?) dissolution of other silicates, probably Al-rich smectites of sedimentary origin that might be present in more argillaceous facies (e.g., interdune facies).

Kaolinite-to-Dickite Diagenetic Transformation

With increasing diagenetic temperature and time, the morphology of kaolin-group minerals steadily evolves from aggregates of books to individual blocky crystals in connection with the modification of their 3-D structure from kaolinite to dickite. In late-stage diagenesis, this structural transformation was first reported in coal basins (Karaganda basin, Kizil basin, Pechora basin) of the former Soviet Union (Kossovskaya and Shutov 1963; Shutov et al. 1970). More recently, Ehrenberg et al. (1993), in basins whose ages range from Late Triassic to Middle Jurassic (Norwegian continental shelf), and McAulay et al. (1994), in Brent Group reservoirs (Northern

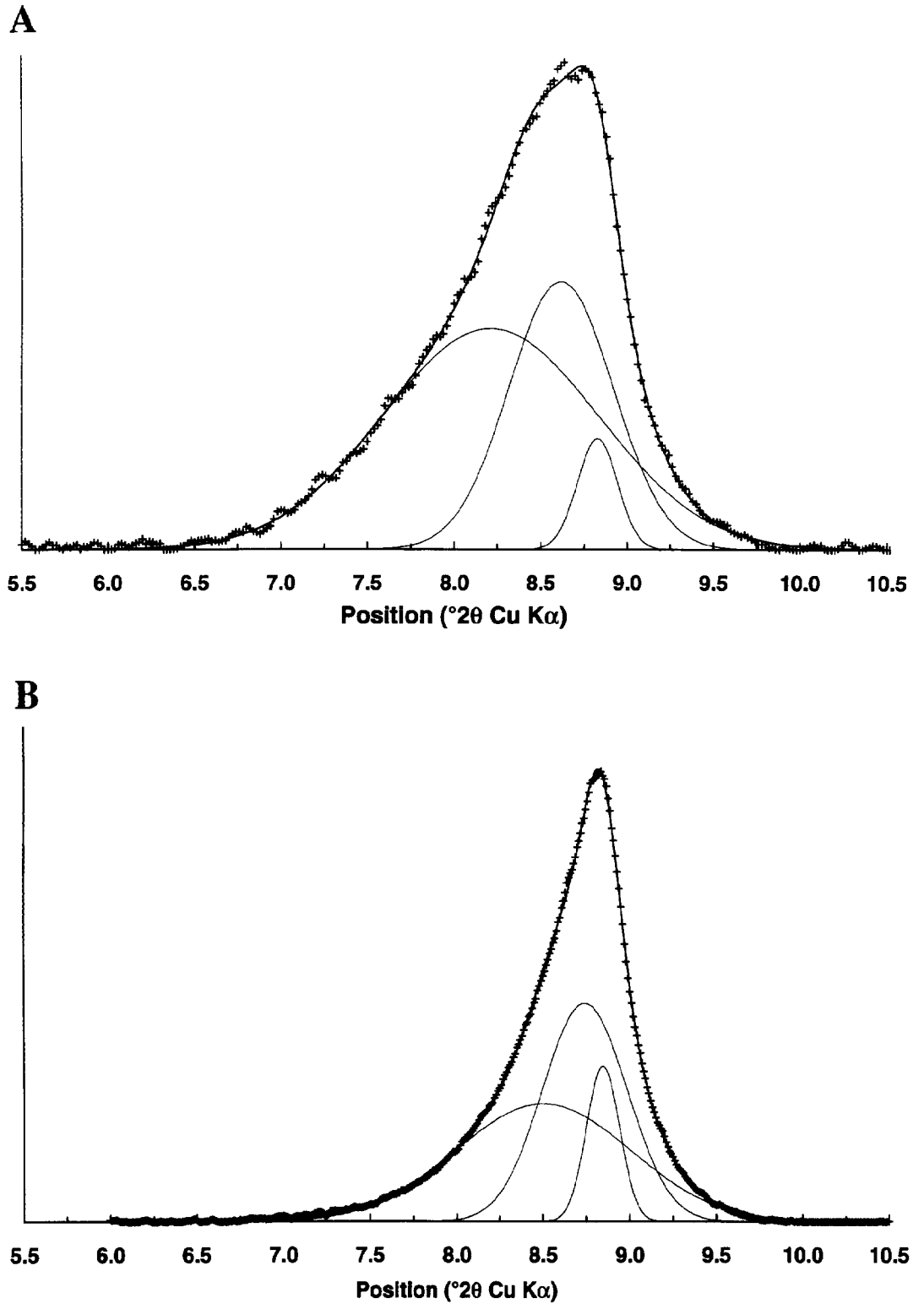

FIG. 11.—Decomposition of the AD profiles (5.5–10.5° 2θ; 16.0–8.4 Å range) shown in Figure 10. **A)** Sample from Well 2 (3321 m), **B)** sample from Well 5 (2968 m).

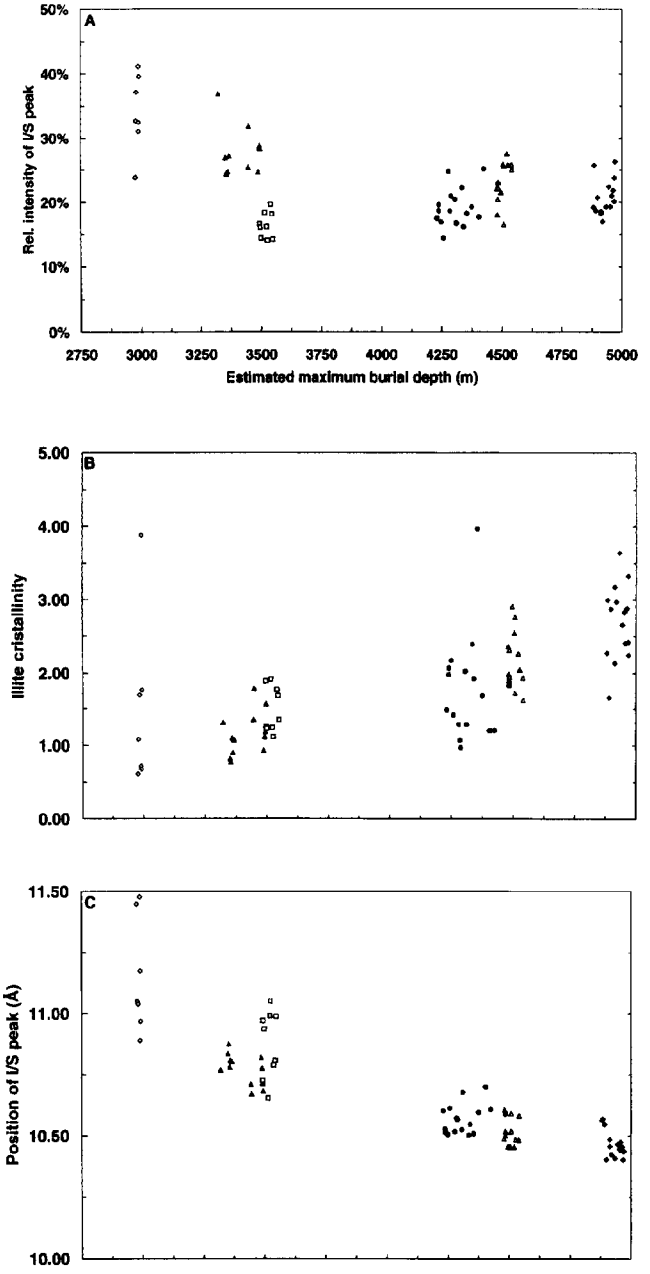

FIG. 12.—Evolution as a function of estimated maximum burial depth; **A)** ordered I/S peak relative intensity (AD; see text for details), **B)** the ordered I/S peak position (AD), obtained from peak decomposition, and **C)** illite crystallinity (see text for details). Open diamonds, Well 1; solid triangles, Well 2; open squares, Well 6; solid circles, Well 3; open triangles, Well 4; solid diamonds, Well 5.

UK), showed a similar transition from vermicular kaolinite to blocky dickite crystals. Because of the very few simultaneous occurrences of kaolinite and dickite, and also because kaolinite crystallinity was not documented, these authors suggested a dissolution and recrystallization process for the kaolinite-to-dickite transformation. On the other hand, Gaupp et al. (1993) showed the coexistence of kaolinite and dickite in the Rotliegend reservoirs of northern Germany. Working on the same basins, Platt (1993) observed both kaolinite and dickite in the shallower samples but only dickite in the deeper wells. We observed the present coexistence of kaolinite and dickite also in our samples, despite the severe alteration of kaolin-group minerals during illitization. Dissolution preferentially affects kaolinite books rather than dickite blocky crystals, probably because of the larger specific surface of the former. Consequently, coexistence of the two polytypes is likely to be restricted to samples in which kaolinite was fairly abundant prior to illitization. This suggests an extended coexistence of kaolinite and dickite, and the very steady character of the kaolinite-to-dickite transition driven by an overall process of minimization of crystal free energy. The progressive kaolinite-to-dickite conversion is indeed superimposed on a preliminary continuous improvement in kaolinite crystallinity (elimination of structural defects; i.e., solid-state minimization of volume free energy). The lack of major morphological changes with the early kaolinite-to-dickite transformation (Fig. 6A, B) seems to indicate a preliminary solid-state transformation similar to the observations by Ruiz Cruz and Moreno Real (1993), who from DTA, infrared spectroscopy, and XRD data, suggested the existence of intermediate structure between kaolinite and dickite, and a progressive "dickitization" of kaolinite with increasing temperature in very low-grade metamorphism. The intermediate dehydroxylation temperature between those of kaolinite and dickite measured on our samples suggests also a structure intermediate between both polytypes (mixed layering?), rather than an effect of increased grain size, which is not observed from SEM. This evolution may correspond to an increasing proportion of BC sequences (dickite is composed of two individual layers with B and C octahedral sites vacant; Drits et al. 1990) within the kaolinite crystallites, which initially contain only B layers. On the other hand, there is undoubtedly a later evolution from dickite pseudomorphs of kaolinite vermicules to dickite blocky crystals (Fig. 6C, D), but this transformation occurs when most of the observed kaolin is dickite. This late evolution is very similar to crystal ripening (dissolution/recrystallization) and could be driven both by elimination of structural defects and by minimization of surface free energy. In the Rotliegend reservoir of the BFB, the progress of this kaolinite-to-dickite transformation reflects thermal and burial histories of the sediments from the time of deposition until the Kimmerian orogenic phase.

Hydrothermal (?) Illitization of Kaolin-Group Minerals

Reasonably consistent K/Ar datings of illitic minerals, as well as lack of a relation between burial depths and K/Ar apparent ages, indicate that the ongoing prograde kaolinite-to-dickite transformation was stopped suddenly: during the Kimmerian orogeny, kaolin-group minerals were destabilized and replaced by illitic minerals. Our K/Ar age of about 155 Ma is very consistent with previous data for Rotliegend sandstone reservoirs throughout the southern North Sea. Lee et al. (1985, 1989) in the Dutch sector, which includes the BFB, and Robinson et al. (1993), Turner et al. (1993), and Ziegler et al. (1994) in the British sector, slightly farther west, have indicated K/Ar ages in the 150–160 Ma range. These consistent data suggest that illitic minerals grow during a relatively short time. Consequently, the crystallochemical structure of illitic minerals reflects the temperature during illitization of kaolin (~ 155 Ma) rather than the progress of a smectite-to-illite transformation. In addition to this evolution of the illite/smectite stacking sequences (decrease in I/S relative abundance, increase in illite content in I/S, and increase in illite mean CSDS) along the c^* axis, the 3-D crystallochemical structure of these illitic minerals evolved from 1M with octahedral *trans* sites vacant (1Mt) to 1M with octahedral *cis* sites vacant (1Mc). This evolution can be related to the morphological changes observed from particles that are essentially fibers to more equant plates: for the 1Mt polytype all the vacant sites are lined up along the unique crystallographic a axis, whereas the availability of two *cis* sites suggests that, for the 1Mc polytype, the vacant sites are lined up along two different crystallographic directions. However, at present there is no direct evidence for strict interdependence between structural and morphological changes. Finally, the increased proportion of 1Mc polytype with the size fraction

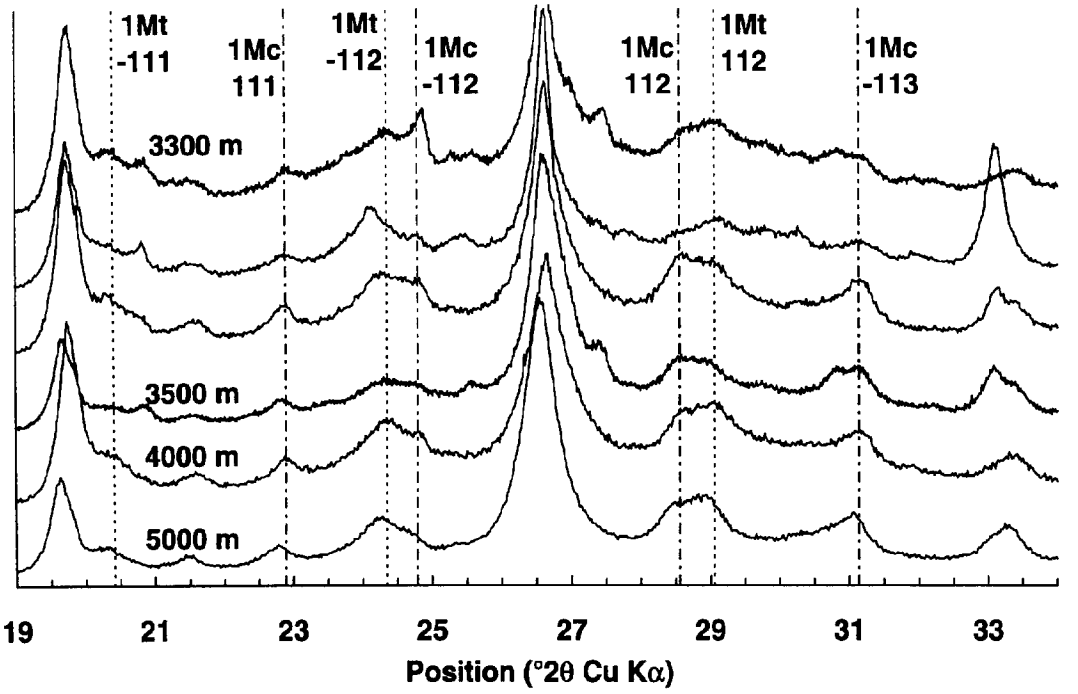

FIG. 13.—Evolution of the 3-D crystallographic structure of illitic material as a function of estimated maximum burial depth. From top to bottom: < 0.2 μm fractions of samples from Well 2 (3350 m, 3445 m, and 3495 m), Well 6 (2893 m), Well 3 (4285 m), and Well 5 (2968 m). Patterns for *cis*- and *trans*-vacant 1M polytypes are same as in Figure 3.

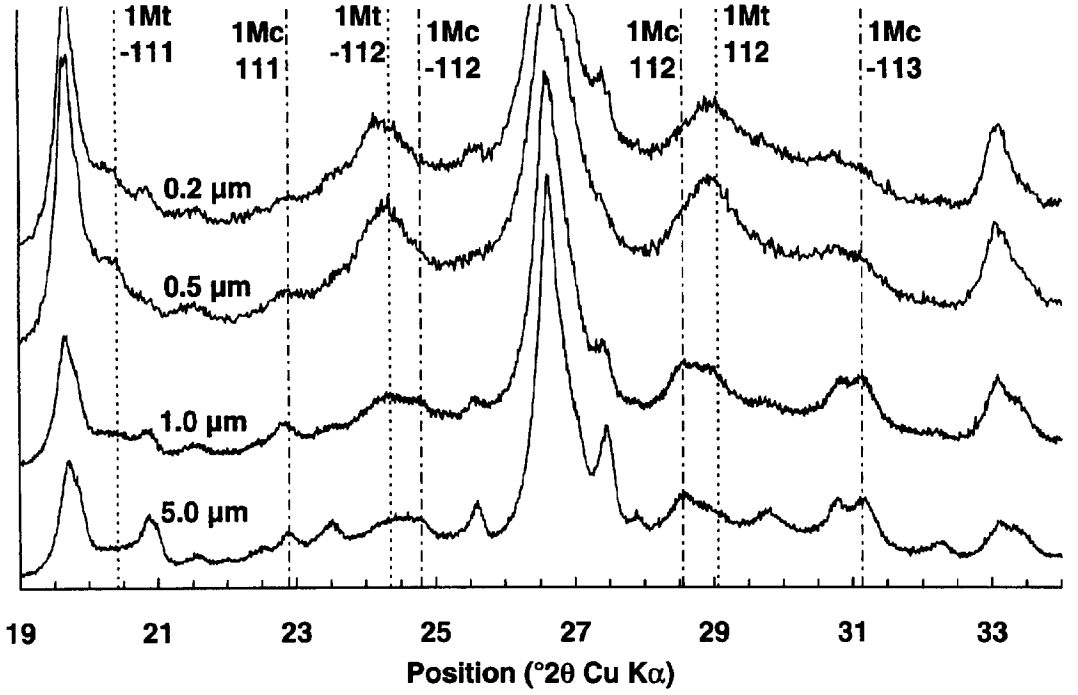

FIG. 14.—Evolution of the 3-D crystallographic structure of illitic material as a function of size fraction. Sample from Well 6 (2893 m). From top to bottom: < 0.2 μm, 0.2–0.5 μm, 0.5–1.0 μm, and < 5.0 μm fractions. Patterns for *cis*- and *trans*-vacant 1M polytypes are same as in Figure 3.

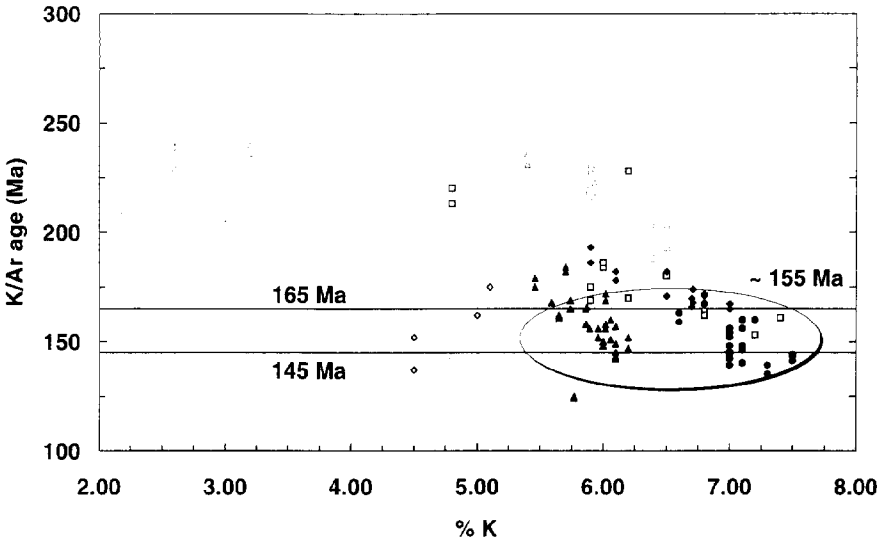

FIG. 15.—K/Ar age as a function of K content for the different size fractions of the six wells studied. Patterns representing the various wells are the same as in Figure 12. Data points obtained from the coarser size fractions of Well 1 samples and from Well 4 samples are grayed because of the large experimental error induced by their low illite contents.

indicates that the phase growing on existing particles (both I/S and illite) is composed of illite layers with 1Mc polytype.

As in the North German Basin (Platt 1993; Gaupp et al. 1993), the time of major illite growth in the BFB is related to major features of the tectonic evolution of the sedimentary basin. In the BFB, illite growth and kaolin destabilization coincide with the Kimmerian orogeny (Late Jurassic to Early Cretaceous) and thus with rifting, extensional faulting, rapid subsidence, and associated increased basal heat flow into the sedimentary pile (Lee et al. 1989; Robinson et al. 1993). The abundance of authigenic illitic minerals increases in the vicinity of graben-bounding faults (Goodchild and Whitaker 1986; Platt 1993). In summary, illitization is a brief process favored both by the high heat flow and by the widespread faulting, which enables significant fluid flow. The nature of the factors responsible for illite crystallization, and the lack of influence of burial, make kaolin illitization a hydrothermal reaction rather than a diagenetic one.

Furthermore, various studies, in agreement with our work, have shown that in Rotliegend sandstone reservoirs illitization occurs mainly at the expense of kaolin-group minerals (Rossel 1982; Lee et al. 1985; Pye and Krinsley 1986). This reaction can be viewed as an exchange of K^+ by H^+:

$$\text{kaolinite} + 2/3\ K^+ \rightarrow 2/3\ \text{illite} + H_2O + 2/3\ H^+ \qquad (2)$$

As emphasized above, the kaolinite-to-illite transformation requires high oversaturation conditions of the end-member illite. Thus, although illite is the only K-bearing silicate to precipitate, both illite and K-feldspar are oversaturated. These conditions prevent K-feldspar from being the source of K^+, and Reaction (2) implies an external source of K^+.

The absence of K-feldspar crystallization reflects the lower degree of saturation of K-feldspar than of illite for a given fluid chemistry. Furthermore, the supply of K^+ has to be balanced by consumption or exportation of H^+ to keep the K^+/H^+ high enough to favor illite precipitation. Also the presence of Fe and Mg in solution, which is induced by dissolution of accessory minerals, both increases the stability field of illite and permits crystallization of illitic I/S rather than pure end-member illite.

Both the above geochemical constraints and the structural characteristics of the illitized zone support the assumption that the kaolinite-to-illite transformation resulted from flow of K^+-rich fluids through the Rotliegend sandstone reservoir of the BFB. Such fluids are assumed to have come from the overlying and laterally adjacent Zechstein evaporite formations, in agreement with previous studies by Rossel (1982), Pye and Krinsley (1986), and Goodchild and Whitaker (1986). Slightly west of the study area, Goodchild and Whitaker (1986) observed intense anhydrite cementation occurring preferentially in the upper part of the reservoir and induced by fluids originating from Zechstein formations, in agreement with sulfur (Sullivan et al. 1994) and oxygen (Sullivan et al. 1994; Ziegler et al. 1994) isotope data from the neighboring Leman field. Additional evidence for the Zechstein origin of the fluids is given by Pye and Krinsley (1986), who detected a significant concentration of Sr in barite, as well as the presence of halite and traces of carnallite in some wells. Chemical analyses of carbonate cement (Pye and Krinsley 1986) also indicate substantial Cu and Zn, which are likely to have come from the Kupferschiefer shales, which lie between Zechstein evaporites and Rotliegend sandstones. Furthermore, the proportion of illitic minerals (relative intensities of illite and kaolin diffraction peaks; Fig. 10) in Wells 4 and 5 is markedly different and is related to the presence of halite, although the structural characteristics of illitic minerals are very similar in these structurally similar wells. This correlation clearly suggests a common Zechstein Formation origin for the fluids responsible for crystallization of halite and for illitization. Consequently, and as suggested by Rossel (1982), Goodchild and Whitaker (1986), and Pye and Krinsley (1986), the main source of ions for illitization of kaolin was probably the overlying Zechstein evaporites, which contain sylvite and polyhalite just west of the study area (Indefatigable Shelf; Ziegler et al. 1994), and not the Carboniferous Coal Measures, as inferred by Gaupp et al. (1993) and Platt (1993), although they observed more intense illitization farther from the Coal Measures formation.

CONCLUDING REMARKS

Despite the variety of burial and thermal histories, the sequence of mineral growth remains broadly constant in the Rotliegend sandstone reservoirs of southern North Sea. The diagenetic sequence of clay minerals in the BFB can be summarized as follows (Fig. 16): (1) from deposition time to the Kimmerian orogeny, crystallization of kaolinite was favored by fluids coming from the underlying Carboniferous Coal Measures source rocks and steady kaolinite-to-dickite transformation; (2) simultaneously with the Kimmerian orogeny, sudden illitization of kaolin-group minerals was favored both by the increased heat flow in the sedimentary pile and by the widespread presence of faults, which permit significant fluid flow from the overlying Zechstein Formation.

Furthermore, in the Broad Fourteens Basin, the structural characteristics of both kaolin-group and illitic minerals are clearly related to the maximum burial depth. The structural characteristics of kaolin-group minerals are related to the burial history of the sediments prior to the Kimmerian orog-

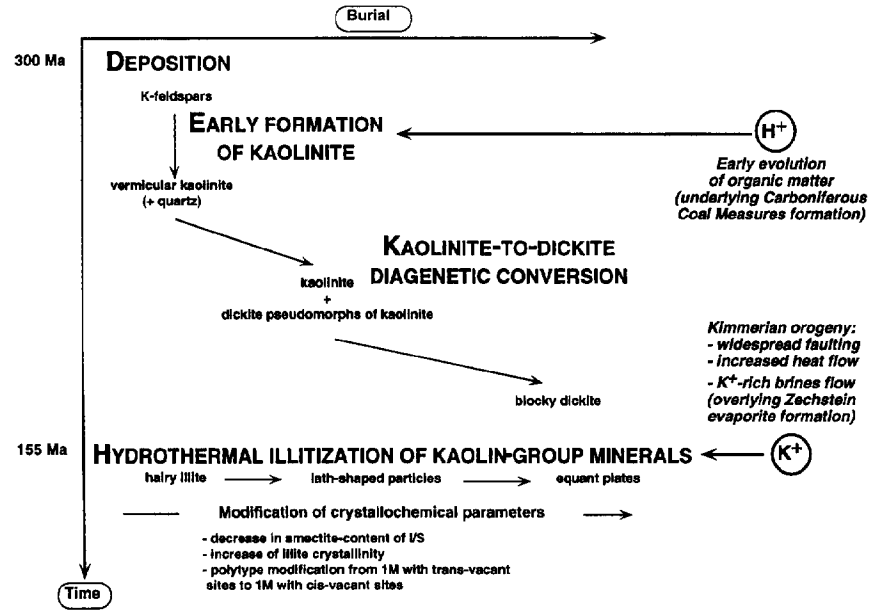

FIG. 16.—Schematic diagram of the reactions affecting clay minerals during burial diagenesis of Rotliegend sandstone reservoir (Broad Fourteens Basin, southern North Sea). The factors controlling the clay mineral reaction, as well as the origin of the fluids, are indicated in italics. The morphological and crystallochemical evolution of clay minerals as a function of maximum burial depth is detailed in smaller characters.

eny, whereas the structure of illitic minerals is related to the temperatures during the Kimmerian orogeny (Fig. 16). The structural characteristics of illitic minerals, i.e., illite content of I/S, ratio of illite to I/S, and 3-D structure of illitic minerals, do not represent the progress of a smectite-to-illite transformation but these characteristics clearly reflect the temperatures during hydrothermal illitization of kaolin (~ 155 Ma).

Successive crystallization and growth of kaolin-group minerals and of illitic minerals both reflect interactions between Rotliegend sandstones and "external" fluids of contrasting origin and characteristics: (1) Acid porewaters, probably expelled from underlying Carboniferous Coal Measures, for dissolution of K-feldspars, crystallization of kaolinite and later kaolinite-to-dickite evolution; and (2) K^+-rich brines, probably from the Zechstein formations, for the kaolin-to-illite reaction.

Clay parageneses and sequences of clay-mineral crystallization observed in the various North Sea reservoirs are very consistent with our study of the Broad Fourteens Basin (see Bjørlykke and Aagaard 1992 for a review of diagenetic schemes proposed for North Sea reservoirs). On the one hand, the diagenetic evolution of clay minerals, as well as the burial history of the Rotliegend sandstone reservoir, are recorded by the progress of the kaolinite-to-dickite conversion, which follows the crystallization of kaolinite at the expense of K-feldspars. On the other hand, in the BFB as well as in most North Sea reservoirs, illitization of kaolin-group minerals is not directly related to burial history. Its timing actually coincides with tectonically active periods with increased heat flow, intense fracturing and faulting, and flows of fluid from an external formation. Consequently, illitization of kaolin-group minerals is to be viewed as a hydrothermal reaction rather than as a diagenetic one. However, in the BFB, as in other Rotliegend sandstone reservoirs from the southern North Sea, an external fluid source for potassium is essential. In other North Sea reservoirs, potassium is usually assumed to be locally derived from K-feldspar, in spite of the high oversaturation conditions for end-member illite, and consequently for K-feldspar, required by the kaolinite-to-illite transformation.

Finally, the widespread character of these transformations emphasizes the need for an accurate characterization of both 1-D and 3-D crystallochemical structure modifications of both kaolin-group and illitic minerals. This characterization requires numerical treatment of experimental XRD profiles and comparison with calculated profiles. Furthermore, in high-porosity systems such as sandstone reservoirs, where crystal growth is not spatially limited, authigenic clay minerals may be fairly large. Consequently, study of the finest clay size fraction must be complemented the with careful examination of coarser size fractions (Towe 1974). Only such careful characterizations of the 1-D and 3-D structures, and of their modifications, performed on all authigenic clay minerals will permit, as a first step, determination of the reaction mechanisms of their diagenetic transformations and, as a second step, modeling of these reactions.

ACKNOWLEDGMENTS

The valuable help of Victor Drits permitted us to interpret correctly these data, which were initially presented during the 30th annual Meeting of the Clay Mineral Society in San Diego, California.

The authors thank also Elf Petroland, Conoco, Arco, Wintershall, and Nam for permission to publish this paper, as well as Richard Hay, Bruce Velde, Alain Meunier, and Steve Hillier for corrections and comments on an early version of the manuscript. Reviewers R. Stephen Fisher and David R. Pevear, Associate Editor Shirley P. Dutton, and Editor John B. Southard are also thanked for their critical reading and correction of the manuscript. Howard May kindly provided kaolinite and dickite reference samples for DTA analysis. Technical support from Elf Aquitaine Production research center in Pau is acknowledged. B.L. and D.B. acknowledge financial support from EAP (Géochimie Minérale laboratory, Pau).

REFERENCES

BAILEY, S.W., 1980, Structures of layer silicates, *in* Brindley, G.W., and Brown, G., eds., Crystal Structures of Clay Minerals and Their X-ray Identification: Mineralogical Society (London), p. 1–123.

BERGER, G., LACHARPAGNE, J.C., VELDE, B., BEAUFORT, D., AND LANSON, B., 1995, Mécanismes et contraintes cinétiques des réactions d'illitisation des argiles sédimentaires déduits de modélisations des interactions eau-roche: Centres de Recherches Exploration-Production Elf Aquitaine, Bulletin, v. 19, p. 225–234.

BJØRLYKKE, K., AND AAGAARD, P., 1992, Clay minerals in North sea sandstones, *in* Houseknecht, D.W., and Pittman, E.D., eds., Origin, Diagenesis, and Petrophysics of Clay Minerals in Sandstones: SEPM Special Publication 47, p. 65–80.

BURLEY, S.D., 1984, Patterns of diagenesis in the Sherwood sandstone group (Triassic), United Kingdom: Clay Minerals, v. 19, p. 403–440.

BURLEY, S.D., AND FLISCH, M., 1989, K-Ar geochronology and the timing of detrital I/S clay illitization and authigenic illite precipitation in the Piper and Tartan fields, Outer Moray Firth, UK North Sea: Clay Minerals, v. 24, p. 285–315.

BURST, J.F., 1969, Diagenesis of Gulf Coast clayey sediments and its possible relation to petroleum migration: American Association of Petroleum Geologists Bulletin, v. 53, p. 73–93.

DRITS, V.A., AND TCHOUBAR, C., WITH THE COLLABORATION OF BESSON, G., BOOKIN, A.S., ROUSSEAUX, F., SAKHAROV, B.A., AND TCHOUBAR, D., 1990, X-Ray Diffraction by Disordered Lamellar

Structures: Theory and Applications to Microdivided Silicates and Carbons: Berlin, Springer-Verlag, 371 p.

DRITS, V.A., WEBER, F., SALYN, A.L., AND TSIPURSKY, S.I., 1993, X-ray identification of one-layer illite varieties: application to the study of illites around uranium deposits of Canada: Clays and Clay Minerals, v. 41, p. 389–398.

DUNOYER DE SEGONZAC, G., 1970, The transformation of clay minerals during diagenesis and low-grade metamorphism: A review: Sedimentology, v. 15, p. 281–346.

EHRENBERG, S.N., AAGAARD, P., WILSON, M.J., FRASER, A.R., AND DUTHIE, D.M.L., 1993, Depth-dependent transformation of kaolinite to dickite in sandstones of the Norwegian continental shelf: Clay Minerals, v. 28, p. 325–352.

FISCHER, M.J., AND JEANS, C.V., 1982, Clay mineral stratigraphy in the Permo-Triassic red bed sequences of BNOC 72/10-1A, Western Approaches, and the south Devon coast: Clay Minerals, v. 17, p. 79–90.

GAUPP, R., MATTER, A., PLATT, J., RAMSEYER, K., AND WALZEBUCK, J., 1993, Diagenesis and fluid evolution of deeply buried Permian (Rotliegende) gas reservoir, northwest Germany: American Association of Petroleum Geologists Bulletin, v. 77, p. 1111–1128.

GLASMANN, J.R., LARTER, S., BRIEDIS, N.A., AND LUNDEGARD, P.D., 1989, Shale diagenesis in the Bergen High area, North Sea: Clays and Clay Minerals, v. 37, p. 97–112.

GLENNIE, K.W., 1972, Permian Rotliegend of northwest Europe interpreted in light of modern desert sedimentation studies: American Association of Petroleum Geologists Bulletin, v. 56, p. 1048–1071.

GOODCHILD, M.W., AND WHITAKER, J.H. MCD., 1986, A petrographic study of the Rotliegendes sandstone reservoir (Lower Permian) in the Rough gas field: Clay Minerals, v. 21, p. 459–477.

GUVEN, N., HOWER, W.F., AND DAVIES, D.K., 1980, Nature of authigenic illites in sandstone reservoirs: Journal of Sedimentary Petrology, v. 50, p. 761–766.

HOFFMAN, J., AND HOWER, J., 1979, Clay mineral assemblages as low grade metamorphic geothermometers: Application to the thrust faulted disturbed belt of Montana, U.S.A., *in* Scholle, P.A., and Schluger, R.P., eds., Aspects of Diagenesis: Society of Economic Paleontologists and Mineralogists Special Publication 26, p. 55–79.

HOWARD, J.J., 1992, Influence of authigenic clay minerals on permeability, *in* Houseknecht, D.W., and Pittman, E.D., eds., Origin, Diagenesis, and Petrophysics of Clay Minerals in Sandstones: SEPM Special Publication 47, p. 257–264.

HOWER, J., ESLINGER, E.V., HOWER, M.E., AND PERRY, E.A., 1976, Mechanism of burial metamorphism of argillaceous sediment: 1. Mineralogical and chemical evidence: Geological Society of America Bulletin, v. 87, p. 725–737.

INOUE, A., 1986, Morphological change in a continuous smectite-to-illite conversion series by scanning and transmission electron microscopies: Chiba University, Journal of the College of Arts and Sciences, v. B-19, p. 23–33.

INOUE, A., KOHYAMA, N., KITAGAWA, R., AND WATANABE, T., 1987, Chemical and morphological evidence for the conversion of smectite to illite: Clays and Clay Minerals, v. 35, p. 111–120.

INOUE, A., VELDE, B., MEUNIER, A., AND TOUCHARD, G., 1988, Mechanism of illite formation during smectite-to-illite conversion in a hydrothermal system: American Mineralogist, v. 73, p. 1325–1334.

KANTOROWICZ, J., 1984, The nature, origin and distribution of authigenic clay minerals from middle Jurassic Ravenscar and Brent group sandstones: Clay Minerals, v. 19, p. 359–375.

KELLER, W.D., REYNOLDS, R.C., AND INOUE, A., 1986, Morphology of clay minerals in the smectite-to-illite conversion series by scanning electron microscopy: Clays and Clay Minerals, v. 34, p. 187–197.

KOSSOVSKAYA, A.G., AND SHUTOV, V.D., 1963, Facies of epi- and metagenesis: International Geology Review, v. 7, p. 1157–1167.

KUBLER, B., 1964, Les argiles, indicateurs de métamorphisme: Institut Français du Pétrole, Revue, v. 19, 1093–1112.

KUBLER, B., 1968, Evaluation quantitative du métamorphisme par la cristallinité de l'illite: état des progrès réalisés ces dernières années: Centre Recherche Pau–Société Nationale des Pétroles d'Aquitaine, Bulletin, v. 2, p. 385–397.

LANSON, B., 1990, Mise en évidence des mécanismes de transformation des interstratifiés illite/smectite au cours de la diagenèse: [unpublished Ph.D. thesis]: Université Paris 6, Jussieu, France, 366 p.

LANSON, B., BEAUFORT, D., BERGER, G., PETIT, S., AND LACHARPAGNE, J.C., 1995, Evolution de la structure cristallographique des minéraux argileux dans le réservoir gréseux Rotliegend des Pays-Bas: Centres de Recherches Exploration-Production Elf Aquitaine, Bulletin, v. 19, p. 243–265.

LANSON, B., AND BESSON, G., 1992, Characterization of the end of smectite-to-illite transformation: Decomposition of X-ray patterns: Clays and Clay Minerals, v. 40, p. 40–52.

LANSON, B., AND CHAMPION, D., 1991, The I/S-to-illite reaction in the late stage diagenesis: American Journal of Science, v. 291, p. 473–506.

LANSON, B., AND MEUNIER, A., 1995, La transformation des interstratifiés ordonnés ($S \geq 1$) illite/smectite en illite dans les séries diagénétiques: Etat des connaissances et perspectives: des Centres de Recherches Exploration-Production Elf Aquitaine, Bulletin, v. 19, p. 149–165.

LANSON, B., AND VELDE, B., 1992, Decomposition of X-ray diffraction patterns: A convenient way to describe complex diagenetic smectite-to-illite evolution: Clays and Clay Minerals, v. 40, p. 629–643.

LEE, M., ARONSON, J.L., AND SAVIN, S.M., 1985, K/Ar dating of time of gas emplacement in Rotliegend sandstone, Netherlands: American Association of Petroleum Geologists Bulletin, v. 69, p. 1381–1385.

LEE, M., ARONSON, J.L., AND SAVIN, S.M., 1989, Timing and conditions of Permian Rotliegende sandstone diagenesis, Southern North Sea: K/Ar and oxygen isotopic data: American Association of Petroleum Geologists Bulletin, v. 73, p. 195–215.

MACKENZIE, R.C., 1970, Simple phyllosilicates based on gibbsite- and brucite-like sheets, *in* Mackenzie, R.C., ed., Differential Thermal Analysis: Volume 1, Fundamental Aspects: New York, Academic Press, p. 497–537.

MCAULAY, G.E., BURLEY, S.D., AND JOHNES, L.H., 1993, Silicate mineral authigenesis in the Hutton and NW Hutton fields: implications for sub-surface porosity development, *in* Parker, J.R., ed., Petroleum Geology of Northwest Europe: Proceedings of the 4th Conference: London, Geological Society of London, p. 1377–1393.

MCAULAY, G.E., BURLEY, S.D., FALLICK, A.E., AND KUZNIR, N.J., 1994, Palaeohydrodynamic fluid flow regimes during diagenesis of the Brent group in the Hutton–NW Hutton reservoirs: Constraints from oxygen isotope studies of authigenic kaolin and reverse flexural modelling: Clay Minerals, v. 29, p. 609–626.

MCHARDY, W.J., WILSON, M.J., AND TAIT, J.M., 1982, Electron microscope and X-ray diffraction studies of filamentous illitic clay from sandstones of the Magnus field: Clay Minerals, v. 17, p. 23–39.

MORRIS, K.A., AND SHEPPERD, C.M., 1982, The role of clay minerals in influencing porosity and permeability in the Bridport sands of Wyth Farm, Dorset: Clay Minerals, v. 17, p. 41–54.

OSBORNE, M., HASZELDINE, R.S., AND FALLICK, A.E., 1994, Variation in kaolinite morphology with growth temperature in isotopically mixed pore-fluids, Brent group, UK North Sea: Clay Minerals, v. 29, p. 591–608.

PERRY, E.A., JR., AND HOWER, J., 1970, Burial diagenesis in Gulf Coast pelitic sediments: Clays and Clay Minerals, v. 18, p. 165–177.

PERRY, E.A., JR., AND HOWER, J., 1972, Late-stage dehydration in deeply buried pelitic sediments: American Association of Petroleum Geologists Bulletin, v. 56, p. 2013–2021.

PLATT, J.D., 1993, Controls on clay mineral distribution and chemistry in the early Permian Rotliegend of Germany: Clay Minerals, v. 28, p. 393–416.

POLLASTRO, R.M., 1985, Mineralogical and morphological evidence for the formation of illite at the expense of illite/smectite: Clays and Clay Minerals, v. 33, p. 265–274.

PYE, K., AND KRINSLEY, D.H., 1986, Diagenetic carbonate and evaporite minerals in Rotliegend aeolian sandstones of the Southern North Sea: Their nature and relationship to secondary porosity development: Clay Minerals, v. 21, p. 443–457.

REX, R.W., 1965, Authigenic kaolinite and mica as evidence for phase equilibria at low temperature: Clays and Clay Minerals, v. 13, p. 95–104.

REYNOLDS, R.C., JR., 1993, Three-dimensional X-ray powder diffraction from disordered illite: Simulation and interpretation of the diffraction patterns, *in* Reynolds, R.C., and Walker, J.R., eds., Computer Applications to X-Ray Powder Diffraction Analysis of Clay-Minerals: Clay Minerals Society Workshop Lectures, v. 5, p. 44–78.

RIGHI, D., AND JADAULT, P., 1988, Improving soil clay minerals studies by high-gradient magnetic separation: Clay Minerals, v. 23, p. 225–232.

ROBINSON, A.G., COLEMAN, M.L., AND GLUYAS, J.G., 1993, The age of illite growth, Village Fields area, Southern North Sea: Evidence from K-Ar ages and $^{18}O/^{16}O$ ratios: American Association of Petroleum Geologists Bulletin, v. 77, p. 68–80.

ROSSEL, N.C., 1982, Clay mineral diagenesis in Rotliegend aeolian sandstones of the Southern North sea: Clay Minerals, v. 17, p. 69–77.

RUIZ CRUZ, M.D., AND MORENO REAL, L., 1993, Diagenetic kaolinite/dickite (Betic cordilleras, Spain): Clays and Clay Minerals, v. 41, p. 570–579.

SCOTCHMAN, I.C., JOHNES, L.H., AND MILLER, R.S., 1989, Clay diagenesis and oil migration in Brent group sandstones of NW Hutton field, UK north sea: Clay Minerals, v. 24, p. 339–374.

SEEMANN, U., 1982, Depositional facies, diagenetic clay minerals and reservoir quality of Rotliegend sediments in the Southern Permian basin (North Sea): A review: Clay Minerals, v. 17, p. 55–67.

SHUTOV, V.D., ALEKSANDROVA, A.V., AND LOSIEVSKAYA, S.A., 1970, Genetic interpretation of the polymorphism of the kaolinite group in sedimentary rocks: Sedimentology, v. 15, p. 69–82.

ŚRODOŃ, J., 1979, Correlation between coal and clay diagenesis in the Carboniferous of the upper Silesian coal basin, *in* Mortland, M.M., and Farmer, V.C., eds., Proceedings of the International Clay Conference, Oxford 1978: Amsterdam, Elsevier, p. 251–260.

ŚRODOŃ, J., 1980, Precise identification of illite/smectite interstratifications by X-ray powder diffraction: Clays and Clay Minerals, v. 28, p. 401–411.

ŚRODOŃ, J., 1981, X-ray identification of randomly interstratified illite-smectite in mixtures with discrete illite: Clay Minerals, v. 16, p. 297–304.

ŚRODOŃ, J., 1984a, Mixed-layer illite-smectite in low-temperature diagenesis: Data from the Miocene of the Carpathian foredeep: Clay Minerals, v. 19, p. 205–215.

ŚRODOŃ, J., 1984b, X-ray powder diffraction of illitic materials: Clays and Clay Minerals, v. 32, p. 337–349.

SULLIVAN, M.D., HASZELDINE, R.S., BOYCE, A.J., ROGERS, G., AND FALLICK, A.E., 1994, Late anhydrite cements mark basin inversion: isotopic and formation water evidence, Rotliegend Sandstone, North Sea: Marine and Petroleum Geology, v. 11, p. 46–54.

THOMAS, M., 1986, Diagenetic sequences and K/Ar dating in Jurassic sandstones, central Viking graben: Effects on reservoir properties: Clay Minerals, v. 21, p. 695–710.

TOWE, K.M., 1974, Quantitative clay petrology: The trees but not the forest?: Clays and Clay Minerals, v. 22, p. 375–378.

TURNER, P., JONES, M., PROSSER, D.J., WILLIAMS, G.D., AND SEARL, A., 1993, Structural and sedimentological controls on diagenesis in the Ravenspurn North gas reservoir, UK Southern North Sea, *in* Parker, J.R., ed., Petroleum Geology of Northwest Europe: Proceedings of the 4th Conference: London, Geological Society of London, p. 771–785.

VELDE, B., SUZUKI, T., AND NICOT, E., 1986, Pressure-temperature-composition of illite/smectite mixed-layer minerals: Niger delta mudstones and other examples: Clays and Clay Minerals, v. 34, p. 435–441.

VELDE, B., AND VASSEUR, G., 1992, A kinetic model of the smectite-to-illite transformation based on diagenetic mineral series: American Mineralogist, v. 77, p. 967–976.

WATANABE, T., 1981, Identification of illite/montmorillonite interstratification by X-ray powder diffraction: Mineralogical Society of Japan, Journal, Special Issue 15, p. 2–41 (in Japanese).
WATANABE, T., 1988, The structural model of illite/smectite interstratified mineral and the diagram for their identification: Clay Science, v. 7, p. 97–114.
WEAVER, C.E., AND BECK, K.C., 1971, Clay water diagenesis during burial: How mud becomes gneiss: Geological Society of America Special Paper 134, 96 p.
VAN WIJHE, D.H., 1987, The structural evolution of the Broad Fourteens Basin, *in* Brooks, J., and Glennie, K., eds., Petroleum Geology of Northwest Europe: Proceedings of the 3rd Conference: London, Graham & Trotman, p. 315–323.
ZIEGLER, K., SELLWOOD, B.W., AND FALLICK, A.E., 1994, Radiogenic and stable isotope evidence for age and origin of authigenic illites in the Rotliegend, Southern North Sea: Clay Minerals, v. 29, p. 555–565.

Received 28 December 1994; accepted 26 September 1995.